NONLINEAR ANALYSIS OF WAVES IN FINITE WATER DEPTH

By

Kyungmo Ahn

A DISSERTATION PRESENTED TO THE GRADUATE SCHOOL
OF THE UNIVERSITY OF FLORIDA IN
PARTIAL FULFILLMENT OF THE REQUIREMENTS
FOR THE DEGREE OF DOCTOR OF PHILOSOPHY

UNIVERSITY OF FLORIDA

1993

ACKNOWLEDGEMENTS

I would like to express my sincere appreciation to Dr. Michel K. Ochi for his continuous guidance and support throughout my Ph.D. program. It has been a tremendous educational experience to study under the supervision of a great scholar who knows how to choose and how to attack challenging problems. The only way I can express my thanks to him will be to do a similar service to my own students in the future. I guess that is the only way we ever thank our teachers.

My thanks are extended to my committee members, Dr. D. Max Sheppard, Dr. Ulrich H. Kurzweg, Dr. Daniel M. Hanes and Dr. Robert J. Thieke, who patiently reviewed this paper. I am also grateful to Dr. Robert G. Dean, Dr. Hsiang Wang and Dr. Ashish J. Mehta for giving valuable input and comments on the dissertation.

The financial support received from the Naval Civil Engineering Laboratory through contract N 47408–91–C–1204 is deeply appreciated.

I am indebted to the staff of the Coastal and Oceanographic Engineering Department, particularly Mr. Subarna Malakar (for his assistance in preparing ARSLOE wave data), Mrs. Helen Twedell and Mr. John Davis (for their assistance in searching the literature), Mrs. Becky Hudson, Mrs. Lucy Hamm, and Mrs. Sandra Bivins (for their excellent teamwork in helping students in every aspects).

The friendship of many colleagues in the department is warmly appreciated. The support and prayers of friends in the Diamond Village bible study group will be cherished forever. I would also like to express my deepest appreciation to my bible teachers, Herbert and Beverly Allen, not only for teaching and sharing scriptures in the weekly bible study, but also for proofreading my dissertation.

My final acknowledgement is reserved for those to whom I probably owe the most. My parents Soo-hahn and Young-Sook Ahn and parents-in-law Doo-Young and Gong-ja Jun have supported me continuously and patiently in all my endeavors. My feelings for them cannot be described by any written word. And it is God's blessing for me to share life with my wife Eunhye and my sons Taewook and Hyunwook in those gloomy days as well as those sunny days.

TABLE OF CONTENTS

ACKNOWLEDGEMENTS ii

LIST OF FIGURES vi

LIST OF TABLES viii

ABSTRACT ix

CHAPTERS

1 INTRODUCTION 1

2 LITERATURE REVIEW 4

- 2.1 Nonlinear Components in Wave Spectra 4
- 2.2 Probability Distributions Applicable to Nonlinear Random Waves 6

3 EVALUATION OF NONLINEARITY IN WAVE SPECTRA 13

- 3.1 Separation of Second-order Spectrum from Measured Spectrum 13
- 3.2 Example of Application 18

4 PROBABILITY DISTRIBUTION OF WAVE PROFILES 29

- 4.1 Application of the Kac-Siegert Method to Probability Distribution of Nonlinear Waves 29
- 4.2 Derivation of Asymptotic Probability Density Function 35
- 4.3 Application of the Probability Density Function to Field Data 41

5 CONCLUSIONS 46

APPENDICES

A KAC-SIEGERT'S METHOD 48

B ARSLOE WAVE DATA 50

C COMPUTATION OF THE BISPECTRUM 52

D INVERSE PRESENTATION OF $Y = U + aU^2$ 54

BIBLIOGRAPHY 58

BIOGRAPHICAL SKETCH 61

LIST OF FIGURES

3.1 Definition of frequency ω_s 15

3.2 Domains for computing $B(\omega_k, \omega_l)$and $B(\omega_l, \omega_k - \omega_l)$ 16

3.3 Portions of wave records measured during the ARSLOE project at locations F710, D625, and D615 where mean water depths are 21.4, 10.1, and 2.1 meters, respectively. 19

3.4 Bicoherence squared spectra at Gage Nos. F710, D625, and D615 with water depths of 21.4, 10.1, 2.1 meters, respectively. 23

3.5 Real part of bispectra at Gage Nos. F710, D625, and D615 with water depths of 21.4, 10.1, 2.1 meters, respectively. 24

3.6 Contour plot of the real part of bispectrum at Gage No. D615 25

3.7 Separation of linear and nonlinear components of spectrum at Gage No. F710 26

3.8 Separation of linear and nonlinear components of spectrum at Gage No. D625 27

3.9 Separation of linear and nonlinear components of spectrum at Gage No. D615 28

4.1 Comparison of probability density function obtained from Kac-Siegert's solution and histogram constructed from data 34

4.2 Comparison between Kac-Siegert and asymptotic probability density functions and histogram constructed from data 38

4.3 Comparison of $Y = U + aU^2$ and $U = (1 - \exp\{-a\gamma Y\})/\gamma a$ for $a = 0.326$ 40

4.4 Comparison of newly developed probability density function and histogram constructed from data at Gage No. D615 43

4.5 Comparison of newly developed probability density function and histogram constructed from data at Gage N0. D625 44

4.6 Comparison of newly developed probability density function and histogram constructed from data at Gage No. F710 45

B.1 Coastal Engineering Research Center (CERC) Field Research Facility, Duck, North Carolina (By courtesy of CERC) 51

D.1 Comparison between $W = V + V^2$ and $V = (1 - \exp\{-\gamma W\})/\gamma$ with $\gamma = 1.28$, $(V, W > 0)$ 57

D.2 Comparison between $W = V + V^2$ and $V = (1 - \exp\{-\gamma W\})/\gamma$ with $\gamma = 3.00$, $(V, W < 0)$ 57

LIST OF TABLES

3.1 Summary of statistics computed from the time histories of surface elevation obtained at Gage Nos. D615, D625, and F710 20

4.1 Parameters computed from the cumulants of surface elevation at Gage Nos. D615, D625, and F710 42

Abstract of Dissertation Presented to the Graduate School
of the University of Florida in Partial Fulfillment of the
Requirements for the Degree of Doctor of Philosophy

NONLINEAR ANALYSIS OF WAVES IN FINITE WATER DEPTH

By

Kyungmo Ahn

August 1993

Chairman: Michel K. Ochi
Major Department: Coastal and Oceanographic Engineering

This dissertation presents the results of a study on the nonlinear stochastic analysis of random waves in finite water depth, in particular, (1) clarification of nonlinearity in wave spectra and (2) development of a probability density function in closed form applicable to wave profiles.

In order to clarify the nonlinear characteristics associated with wave-wave interactions, which are particularly pronounced for waves in finite water depth, a method is developed to examine those frequencies having nonlinear energy components and their magnitudes. The nonlinear components of the spectral density at a specified frequency are considered to be the accumulation of nonlinear interactions associated with various pairs of two frequency components. Here, interaction includes not only the sum but also the difference of two frequencies. The separation of the nonlinear component of the energy density of a spectrum is achieved by applying the concept of the bicoherence spectrum.

The separation procedure is applied to wave spectra computed from data obtained in the ARSLOE Project during storm. The results demonstrate that nonlinear components are present at low and high frequencies but no nonlinear components exist in the neighborhood of the frequency where the spectrum peaks and that the ratio of nonlinear energy to the total energy increases significantly with a decrease in water depth.

In order to evaluate the statistical properties of nonlinear waves, a probability density function applicable to non-Gaussian random waves is developed in closed form. Currently, no probability density function in closed form representing non-Gaussian random processes is available.

In the derivation of the probability density function, the concept of Kac-Siegert's method developed for nonlinear mechanical system is applied. That is, the Kac-Siegert formula is asymptotically expressed in terms of a random variable that obeys a normal distribution with parameters evaluated from information on cumulants of the wave record. Then, by applying the transformation technique of random variables, the desired probability density function is developed in closed form. Comparisons between the newly developed probability density function and the histograms constructed from wave records at various water depths obtained in the ARSLOE Project during storm show excellent agreement.

CHAPTER 1
INTRODUCTION

The characteristics of waves in finite water depth are significantly different from those of waves in deep water. Visibly, waves in finite water depth show a trend of skewness in their profile, and the degree of skewness is pronounced in severe seas in shallow water. This is attributed to a nonlinear wave-wave interaction (namely, energy transfer) between component waves.

Although many studies on the nonlinear characteristics of ocean waves have been carried out to date, little research has been made on nonlinear stochastic properties of waves. Those studies are primarily based on the perturbation expansion for a random sea of constant finite depth such as the weakly nonlinear random waves derived from the Stokes' expansion of governing equation using potential theory (Tick 1959, 1961, Phillips 1960, 1961, Hasselmann 1962, 1963a, 1963b, Longuet-Higgins 1963). The weakly nonlinear wave theory has provided significant insight on nonlinear wave-wave interactions; however, the theory cannot account for steep waves or waves in shallow water that show strong nonlinearity.

It is of considerable interest to understand nonlinearity involved in the spectra of waves in finite water depth. Several studies on the quantitative estimation of nonlinear spectral energy components of ocean waves have been conducted (Masuda et al. 1979, Hudspeth and Chen 1979, etc.). However, almost all these studies have been based on weakly nonlinear random waves, which are obviously insufficient to explain nonlinearity in the spectra of waves in finite water depth.

Another important and interesting study on nonlinear characteristics of waves in finite water depth is the probability distribution of the wave profile. Currently available probability density functions representing non-Gaussian characteristics of wave profiles in finite water depth have drawbacks. For example, the probability density functions given in series form (Gram-Charilier prob. distribution) have negative values at some part of the distribution. The probability density functions developed based on the weakly nonlinear wave theory cannot be applied to waves having strong non-Gaussian characteristics (Tayfun 1980, Huang et al. 1983, Langley 1987).

This study adresses nonlinear characteristics of waves in finite water depth, in particular, (1) clarification of the nonlinearity in wave spectra and (2) development of a probability density function in closed form that is applicable to surface elevation of waves in finite water depth.

In order to clarify the nonlinearity in wave spectra, a bispectral analysis technique is applied for quantitative evaluation of nonlinear wave-wave interactions. When various spectral components interact with one another due to nonlinearities, the resulting components are phase coherent with the primary components. Therefore, those components are not considered to be statistically independent. The bispectrum, which measures the statistical dependence of three spectral components whose sum frequncy is zero, may therefore be a useful tool to investigate the nonlinearities of random waves in finite water depth. By applying the concept of a bicoherence spectrum, a method to separate the nonlinear component of the energy density of spectrum will be developed.

In the derivation of a probability density function applicable to nonlinear wave profiles, the concept of the Kac-Siegert method (Appendix A) for evaluating the response of a nonlinear mechanical system is applied. The background of the application is as follows:

It is commonly known that the response of a nonlinear system is generally a non-Gaussian random process, even if the input of the system is a Gaussian random process. The response of a nonlinear system is often presented by Volterra's stochastic series expansion, and Kac-Siegert derived the probability distribution of the response with knowledge of the second-order frequency response function.

Now, let us consider wave profiles in the ocean. The results of statistical analysis of waves obtained during the Atlantic ocean Remote Sensing Land-Ocean Experiment (ARSLOE) Project (Ochi et al. 1983) have shown that the profile of offshore waves follows the normal probability distribution, while the wave profile near shoreline obeys the Gram-Charlier series (non-Gaussian) distribution. This implies that wave characteristics are changing from a Gaussian random process to a non-Gaussian random process with decreasing water depth. This situation resembles the response of a nonlinear mechanical system which is a non-Gaussian random process whose skewness increases with increase in degree of nonlinearity. The concept of Kac-Siegert's method which yields the probability density function of a nonlinear response may therefore be applied to the problem at issue. However, the second-order frequency response function necessary to apply the method is unknown for nonlinear waves. Hence, we will develop an analytical method to derive Kac-Siegert's solution from only a knowledge of nonlinear wave data through separating wave spectra into linear and nonlinear components.

The paper consists of three chapters followed by conclusions and appendices. Chapter 2 reviews currently available literature on nonlinear components in wave spectra as well as the probability distributions applicable to surface elevation of nonlinear random waves.

Chapter 3 presents a method to identify second-order spectrum representing the nonlinear properties in energy spectrum computed from measured wave data. The method is applied to field data obtained in the ARSLOE Project during storm.

Chapter 4 presents the derivation of the probability density function in closed form applicable to random waves in finite water depth, which is considered to be a non-Gaussian random process. By applying the concept of Kac-Siegert's method, a new probability density function is derived in closed form and is compared with histograms constructed from measured wave data.

Chapter 5 presents the findings and conclusions obtained from the present study.

The appendices outline (A) Kac-Siegert's method, (B) ARSLOE wave data, (C) the computational procedure of bispectrum, and (D) inverse presentation of $Y = U + aU^2$.

CHAPTER 2
LITERATURE REVIEW

This chapter reviews literature on nonlinear components in wave spectra and the probability distributions applicable to nonlinear random waves, which usually can be considered as a non-Gaussian random process.

2.1 Nonlinear Components in Wave Spectra

The perturbation expansion (or Stokes' expansion) method to the governing equations of inviscid fluid and incompressible, irrotational flow has been extended to random sea waves by Tick (1959, 1961), Phillips (1960, 1961), Hasselmann (1962, 1963a), and Longuet-Higgins (1963). Hereafter, the solution obtained from the Stokes' expansion method for random waves in finite water depth will be denoted as the weakly nonlinear solution.

Tick's derivation of the weakly nonlinear solution extended to the second order, and he presented the second-order interaction kernel for random waves in finite water depth (1959, 1961). Hasselmann (1962) carried out the perturbation to the third order in spectral energies, E_6, and found that the spectral energy, E, could be represented in a perturbation series as follows:

$$E = E_2 + E_4 + E_6 + \cdots \tag{2.1}$$

where

E_2 = linear spectrum, spectral energy due to linear components

E_4 = second-order spectrum

E_6 = third-order spectrum

The perturbation terms of odd order all vanish for a Gaussian zero mean varible.

$$E_3 = E_5 = \cdots = 0 \tag{2.2}$$

Since the spectrum obtained from measured wave data contains both linear and nonlinear higher order spectral energy components, it is often necessary to separate the spectral energy of linear components from the measured spectrum. Hereafter, the spectrum obtained from measured data will be denoted as the measured spectrum.

The second-order spectrum $S_2(\omega)(= E_4)$ is given by the following convolution integral (Tick 1961, for example).

$$S_2(\omega) = \int_{-\infty}^{\infty} |K(\omega_k, \omega)|^2 S_1(\omega - \omega_k) S_1(\omega_k) d\omega_k \tag{2.3}$$

where

$S_1(\omega_k) = E_2 =$ linear spectrum
$K(\omega_k, \omega) =$ second-order interaction kernel
$\omega_k,\ \omega =$ radian frequency

Many studies have been conducted to separate the second-order spectrum from the measured spectrum. As shown in Eq. 2.3, the kernel function and linear spectrum should be given to compute the second-order spectrum. Most of the studies reviewed here employed the second-order interaction kernel obtained from the weakly nonlinear solution. Since the linear spectrum $S_1(\omega)$ in Eq. 2.3 is unknown in advance, each method has a different approach in assuming the first-order spectrum.

The first attempt to compute the second-order spectrum was made by Tick (1959, 1961). In the derivation of the second-order weakly nonlinear solution, he computed the second-order spectrum by assuming that the linear spectrum was given. Hamada (1965) made a correction to Tick's solution. To obtain the second-order spectrum from the measured spectrum in the wave tank, he assumed the approximate shape of the linear spectrum by excluding the part that appeared to be the obvious nonlinear part from the measured spectrum. In order to compute the second-order spectrum, Hudspeth and Chen (1979) employed both theoretical spectra and a smoothed measured spectrum estimated from wave data obtained during Hurricane Carla. Masuda et al. (1979) developed the iterative method for the separation of the second-order spectrum from the measured spectrum. They assumed that the measured spectrum consisted of linear and second-order spectrum. Using the measured spectrum as an initial estimation for the linear spectrum, they could separate the second-order spectrum within a few iterations.

The methods for obtaining the second-order spectrum reviewed above are all based on the second-order interaction kernel of weakly nonlinear solution. Therefore, as stated in Chapter 1, these methods are not applicable to random waves having strong non-Gaussian characteristics.

On the other hand, Kim and Power (1979) utilized bispectral analysis to investigate the nonlinear wave-wave interactions of coherent waves in plasma fluctuation data. In particular, Kim and Power successfully showed that the bicoherence spectrum might be used to discriminate between nonlinearly coupled waves and linear free waves. Furthermore, the bicoherence squared was shown to measure the fraction of wave energy due to the second-order wave coupling in a measured spectrum. However, they considered only the case of single three wave coupling and did not apply the technique to the separation of the second-order spectrum from the measured spectrum.

The bispectral analysis technique by Kim and Power (1979) will be reviewed in detail in Chapter 3 because the technique can be used for identifying the nonlinear components of random waves having strong non-Gaussian characteristics.

2.2 Probability Distributions Applicable to Nonlinear Random Waves

One of the early attempts to represent the probabilistic distributions of the surface elevation of nonlinear random waves was made by Kinsman (1960) by means of a Gram-Charlier probability density function. The Gram-Charlier probability density function was developed by applying the concept of orthogonal polynomials with respect to the probability density function. Since Hermite polynomials are orthogonal with respect to the Gaussian (normal) distribution, the probability density function can be expressed as a function of

Gaussian distribution and a series of Hermite polynomials. The Gram-Charlier series of Type A probability density function for a standardized random variable is as follows:

$$\begin{aligned} f(z) &= \frac{1}{\sqrt{2\pi}}e^{-\frac{z^2}{2}}\left[1+\frac{m_3}{3!}H_3(z)+\frac{m_4-3}{4!}H_4(z)+\frac{m_5-10m_3}{5!}H_5(z)\right. \\ &+ \left.\frac{m_6-15m_4+30}{6!}H_6(z)+\cdots\right] \end{aligned} \quad (2.4)$$

where

z = standardized random variable

m_j = j-th moment of the standardized random variable

$H_n(z)$ = Hermite polynomials of degree n

Significant advances in theoretical analysis of nonlinear random waves were made in the late 1950s and early 1960s by Tick (1959, 1961), Phillips (1960, 1961), Hasselmann (1962, 1963a, 1963b), and Longuet-Higgins (1963). Longuet-Higgins (1963) specifically investigated the effects of nonlinearities on the statistical distribution of random waves. He derived a series probability density function through the cumulant-generating function. The distribution was expressed in terms of cumulants as follows:

$$\begin{aligned} f(y) &= \frac{1}{\sqrt{2\pi}\sigma}e^{-\frac{y^2}{2\sigma^2}}\left[1+\frac{\lambda_3}{3!}H_3(\frac{y}{\sigma})+\frac{\lambda_4}{4!}H_4(\frac{y}{\sigma})+\frac{\lambda_5}{5!}H_5(\frac{y}{\sigma})\right. \\ &+ \left.\left(\frac{\lambda_6}{6!}+\frac{\lambda_3^2}{72}\right)H_6(\frac{y}{\sigma})+\cdots\right] \end{aligned} \quad (2.5)$$

where

σ^2 = variance of y

$\lambda_3 = k_3/k_2^{\frac{3}{2}}$ = skewness

$\lambda_4 = k_4/k_2^2$ = kurtosis $- 3$

$\lambda_5 = k_5/k_2^{\frac{5}{2}}$

k_j = cumulants

This expression proved to be in the same form as the Edgeworth series distribution (1905) and also the modified form of the Gram-Charlier probability density function. Therefore, the Gram-Charier, Edgeworth, and Longuet-Higgins probability density functions were essentially the same form, although their approaches were entirely different. Detailed comparisons and derivations of these three probability density functions were presented by Ochi (1985).

As is shown in Eq. 2.5, the first term is the normal distribution and the remaining terms represent the effects of non-Gaussian characteristics. This probabilty density function, however, has a drawback. Since the distribution is given in series form, it usually has a negative value at some part of the distribution caused by a finite number of terms in computing the density function. Ochi and Wang (1984a) applied the probability density function to wave records measured at various water depths during the growing stage of a storm and concluded that

- the series is not uniformly convergent; in other words, the inclusion of higher order terms does not necessarily give more accurate results, and
- the probability distribution that includes the parameter λ_3 (skewness) only agrees relatively well with the histogram, in general.

Another approach for deriving the probability distributions applicable to nonlinear random waves is from the weakly nonlinear solution. A second-order random wave may be expressed in the following form:

$$y(t) = Re\sum_{k=1}^{N} c_k\, e^{i\phi_k} + Re\sum_{k=1}^{N}\sum_{l=1}^{N} c_k c_l \left\{ q_{kl} e^{i(\phi_k+\phi_l)} + r_{kl} e^{i(\phi_k-\phi_l)} \right\} \tag{2.6}$$

where

$\phi_k = \omega_k t + \epsilon_k$ = phase function

t = time

$\omega_k = 2\pi k/T$ = radian frequency

T = record length of time series

ϵ_k = uniformly distributed random phase

q_{kl} is a coefficient associated with $\omega_k + \omega_l$, which is the sum of the interactions between two frequency components ω_k and ω_l, while r_{kl} is associated with the difference of interactions between ω_k and ω_l. These interaction coefficients are functions of ω_k, ω_l, and the water depth. Eq. 2.6 has been used extensively for the digital simulation of nonlinear random waves (Hudspeth and Chen, 1979; Sharma and Dean, 1979; Anastasiou et al., 1982; Tuah and Hudspeth, 1985) and for statistical analysis (Tayfun, 1980; Langley, 1987).

Tayfun (1980) developed the probability density function applicable to nonlinear random waves observed in deep water. Assuming the spectrum was narrow-banded, he developed from Eq. 2.6 the following amplitude modulated Stokes waves:

$$y(x,t) = a(x,t)\cos(\chi_0 + \varepsilon) + \frac{1}{2}k_0 a^2(x,t)\cos 2(\chi_0 + \varepsilon) + \cdots \tag{2.7}$$

where

x = horizontal axis

k_0 = ω_0^2/g = wave number

ω_0 = mean frequency

g = gravitational acceleration

Tayfun assumed that the slowly varying amplitude $a(x,t)$ and the phase ε follow the Rayleigh and uniform probability distributions, respectively, and derived the marginal cumulative distribution of surface elevation, $F(y)$, by applying the technique of transformation of random variables. However, the cumulative distribution $F(y)$ and the probability density function $f(y)$ require numerical integration. Therefore, the probability density function is not in closed form.

Huang et al. (1983) also studied nonlinear characteristics of waves and extended Tayfun's analysis to the third order by using regular Stokes waves in deep water as follows:

$$y(x,t) = \frac{1}{2}a^2k + a\cos\chi + \frac{a^2k}{2}\cos 2\chi + \frac{3a^3k^2}{8}\cos 3\chi + \cdots \tag{2.8}$$

By using the narrow-band assumption and by analogy with Tayfun's derivation, they assumed amplitude a and phase χ to be slowly varying functions. Then, by transformation of random variables with successive approximations, the probability density function of the surface elevation was derived. In precisely the same manner as in the deep water case, Huang et al. (1983) derived the probability density function of the surface elevation in finite water depth by extending the method to the Stokes waves of the third order in finite water depth, which was given by Bowden (1948) as follows:

$$\begin{aligned} y &= \frac{a^2k}{2}\coth kd + a\cos\chi \qquad (2.9)\\ &+ \frac{a^2k}{2}\coth kd\left(1+\frac{3}{2\sinh^2 kd}\right)\cos 2\chi \\ &+ \frac{3a^3k^2}{8}\left(1+\frac{3}{\sinh^2 kd}+\frac{3}{\sinh^4 kd}+\frac{9}{8\sinh^6 kd}\right)\cos 3\chi \end{aligned}$$

where d is the water depth. Huang et al. found that the probability density function derived for deep water waves depended on two parameters: the root-mean-square surface elevation and the significant slope. For waves in finite water depth, an additional parameter, the nondimensional depth, was also required.

Langley (1987) presented the probability distribution of second-order random waves in finite-water depth without the narrow-band assumption. In the development of the density function of wave profiles, he first represented the second-order random waves of Eq. 2.6 in the following form by using the technique developed by Kac and Siegert (1947) for the statistical analysis of nonlinear systems.

$$y(t) = \sum_j(\beta_j Z_j + \lambda_j Z_j^2) \tag{2.10}$$

where Z_j is a standardized normal random variable. The parameters β_j and λ_j are evaluated from matrices obtained from the weakly nonlinear solution.

Since $y(t)$ is represented in terms of the standardized normal random variable Z_j, the probability density function of $y(t)$ can be derived through the characteristic function of Eq. 2.10, but the probability density function is not expressed in closed form.

It should be noted that the probability density functions derived by Tayfun (1980), Huang et al. (1983), and Langley (1987) from the weakly nonlinear solution are generally not applicable to steep waves or shallow-water waves. This is because the probability density function was derived from the solution of the Stokes expansion method, which is valid only for weakly nonlinear and nonresonant waves. For example, the second-order solution represented in Eq. 2.6 becomes divergent without bound in shallow water where the resonant condition is easily satisfied for second-order wave-wave interactions.

Recently, Cieślikiewicz (1990) applied the maximum entropy method to nonlinear random waves. The maximum entropy method has often been considered in determining the probability density function of a random variable from data in which information on the statistical distribution has been inadequate. The principle of the method is that the probability distribution that maximizes the entropy function subject to moments constraints has the least biased statistical information (Jaynes, 1957; Dowson and Wragg, 1973; Sobczyk and Trebicki, 1990). For given moments up to fourth order evaluated from data, Cieślikiewicz derived the probability density function numerically by solving the system of nonlinear integral equations. Although the results showed good agreement with field data, the approach was essentially a data fitting technique. One should also note that the probability density function does not exist when moments of data only up to third order (variance and skewness) are available.

As this brief review of the literature indicates, most studies on nonlinear components in wave spectra have employed the weakly nonlinear solution as a tool to investigate nonlinearities in random waves in finite water depth. This approach is valid only for slightly non-Gaussian processes. The bispectral analysis technique has proven to be a useful tool for identifying nonlinear components in random waves and will be used in this paper for the statistical analysis of random waves in finite water depth.

Several probability density functions have been proposed to represent the non-Gaussian characteristic of a random sea surface. The Gram-Charlier, Edgeworth, and Longuet-Higgins probability density functions are essentially the same form and have negative value at some part of the distribution. The probability density functions developed based on the analytic solution of Stokes perturbation method are generally not applicable to steep waves or shallow-water waves. The probability density function obtained by applying the maximum entropy method is essentially a data fitting technique. In short, probability density functions applicable to nonlinear random waves having strong non-Gaussian characteristics have not been analytically developed to date.

CHAPTER 3
EVALUATION OF NONLINEARITY IN WAVE SPECTRA

This chapter consists of two sections. The first section presents the method to separate the second-order spectrum representing nonlinear properties from measured spectrum. A method for evaluating wave-wave interaction between two specified frequencies developed by Kim and Power (1979) is applied to nonlinear interactions associated with various pairs of frequency components in the wave spectrum.

The second section presents sample application. The method developed is applied to field data obtained during the growing stage of a storm in the ARSLOE project. The results of the analysis and a discussion on nonlinear characteristics of random waves in different water depths are presented.

3.1 Separation of Second-order Spectrum from Measured Spectrum

In this study, the time history of a wave profile divides into linear and second-order part as follows:

$$y(t) = y_1(t) + y_2(t) \tag{3.1}$$

Let us first consider the interaction associated with two frequency components ω_k and ω_l, which are arbitrarily chosen constant frequencies. In this case, Kim and Power (1979) derived the interaction in the spectral density at a frequency ω_m (where ω_m is the sum of ω_k and ω_l) as follows:

$$S(\omega_m) = E\left[|Y_L(\omega_m)|^2\right] + \frac{|B(\omega_k,\omega_l)|^2}{E\left[|Y(\omega_k)\,Y(\omega_l)|^2\right]} \tag{3.2}$$

where

$Y_L(\omega_m)$ = Fourier transform of the linear component $y_1(t)$ at the frequency ω_m

$Y(\omega_k)$, $Y(\omega_l)$ = Fourier transform of the wave profile $y(t)$ at the frequencies ω_k and ω_l, respectively

$B(\omega_k, \omega_l)$ = bispectral density function

The first term of Eq. 3.2 represents the spectral density of the linear component $y_1(t)$ at the frequency ω_m, while the second term represents that of the nonlinear component. By multiplying $S(\omega_m) = E[|Y(\omega_m)|^2]$ to the numerator and denominator, respectively, of the second term of Eq. 3.2, we may write

$$\begin{aligned} S(\omega_m) &= E\left[|Y_L(\omega_m)|^2\right] + \frac{|B(\omega_k,\omega_l)|^2}{E\left[|Y(\omega_k)Y(\omega_l)|^2\right]\; E\left[|Y(\omega_m)|^2\right]} S(\omega_m) \\ &= E\left[|Y_L(\omega_m)|^2\right] + b^2(\omega_k,\omega_l)\cdot S(\omega_m) \end{aligned} \tag{3.3}$$

where

$$b(\omega_k,\omega_l) = \left\{ \frac{|B(\omega_k,\omega_l)|^2}{E\left[|Y(\omega_k)Y(\omega_l)|^2\right]\; E\left[|Y(\omega_m)|^2\right]} \right\}^{\frac{1}{2}} \tag{3.4}$$

$b(\omega_k, \omega_l)$ in the above equation is called the bicoherence spectrum, and its squared quantity indicates the fraction of the spectral density considered as a nonlinear component.

In applying Kim and Power's method to the present problem, we consider the frequency ω_k and ω_l not to be constant; instead, they are variables. This implies that the nonlinear component of the spectral density at a frequency ω_m is equal to the accumulation of nonlinear interactions associated with various pairs of frequency components ω_k and ω_l under the condition that $\omega_k + \omega_l = \omega_m$. Furthermore, we consider the interactions that occurs not only at the frequency $(\omega_k + \omega_l)$ but also at the frequency $(\omega_k - \omega_l)$, where $\omega_k > \omega_l$. The latter is equivalent to the interaction between ω_l and $(\omega_k - \omega_l)$. In evaluating the interaction at the frequency $(\omega_k - \omega_l)$, it is assumed that the spectral energy density at frequencies smaller than the minimum frequency of the main energy density in the spectrum (ω_s in Figure 3.1) is due to the nonlinear interaction associated with the difference between various combinations of the two frequency components at ω_k and ω_l. The spectral density

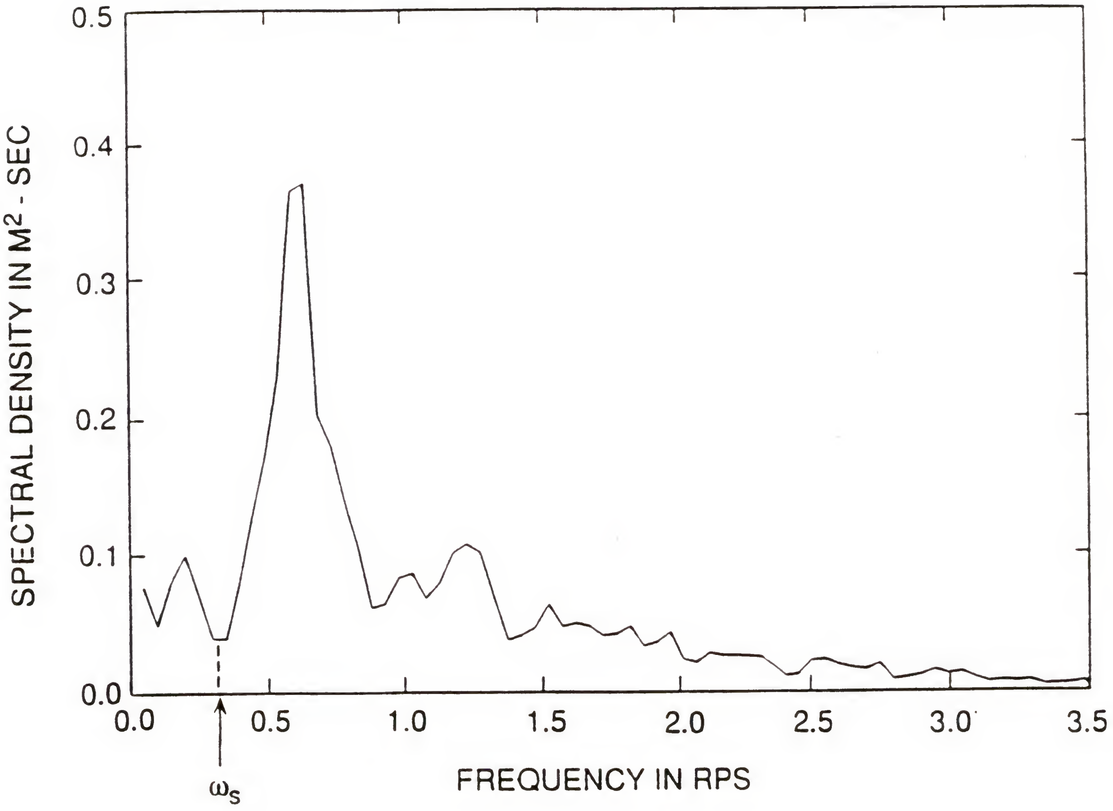

Figure 3.1: Definition of frequency ω_s

for frequencies greater than ω_s is due to the nonlinear interaction associated with the sum of various combinations of two frequency components.

Let us evaluate the interaction due to the sum of two frequency components. We may write the Fourier transform of $y(t)$ at the frequency ω_m as follows:

$$Y(\omega_m) = Y_L(\omega_m) + \sum_{\omega_k+\omega_l=\omega_m} A_L(\omega_k,\omega_l)\, Y_L(\omega_k)\, Y_L(\omega_l) \tag{3.5}$$

Note that the summation is for various combinations of components at ω_k and ω_l where $\omega_k+\omega_l = \omega_m$, and the second term of Eq. 3.5 is a convolution in discrete form. The coupling coefficient $A_L(\omega_k,\omega_l)$ can be obtained by multiplying each side of Eq. 3.5 by $Y_L^*(\omega_k)$ and

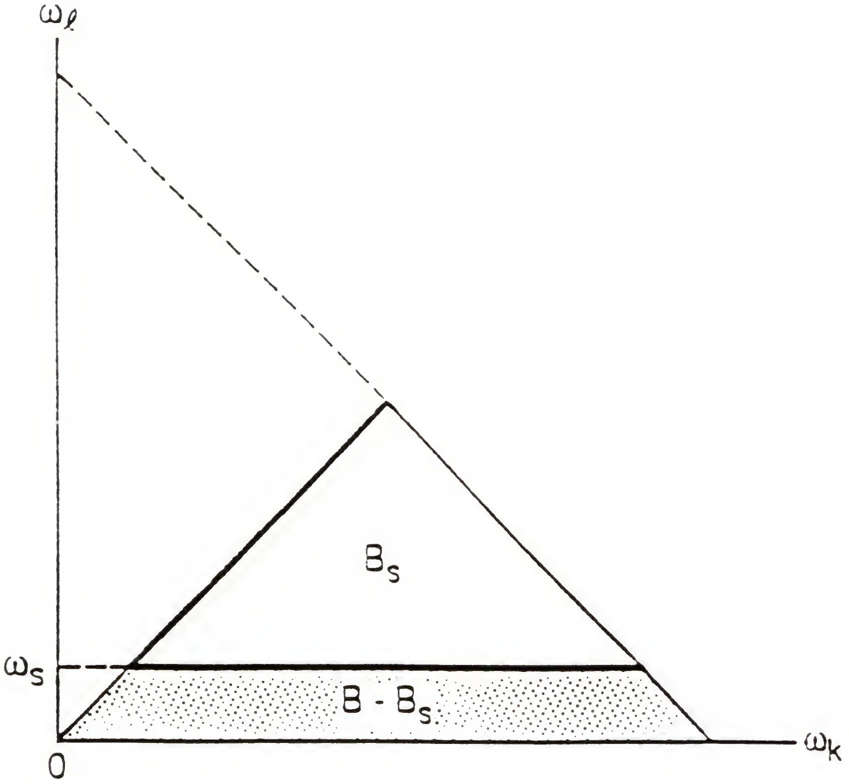

Figure 3.2: Domains for computing $B(\omega_k, \omega_l)$and $B(\omega_l, \omega_k - \omega_l)$

$Y_L^*(\omega_l)$ and by taking the expected value. That is,

$$A_L(\omega_k,\omega_l) = \frac{B^*(\omega_k,\omega_l)}{E\left[|Y_L(\omega_k)Y_L(\omega_l)|^2\right]} \tag{3.6}$$

where $B^*(\omega_k,\omega_l) =$ complex conjugate of the bispectrum $B(\omega_k,\omega_l)$. It should be noted that the domain of the bispectrum in this case is limited in B_s as indicated in Figure 3.2.

The spectral density function at the frequency ω_m can be obtained from Eqs. 3.5 and 3.6 as

$$\begin{aligned} S(\omega_m) &= E\left[|Y_L(\omega_m)|^2\right] + \sum_{\omega_k+\omega_l=\omega_m} |A_L(\omega_k,\omega_l)|^2 \cdot E\left[|Y_L(\omega_k)Y_L(\omega_l)|^2\right] \\ &= E\left[|Y_L(\omega_m)|^2\right] + \sum_{\omega_k+\omega_l=\omega_m} \frac{|B(\omega_k,\omega_l)|^2}{E\left[|Y_L(\omega_k)Y_L(\omega_l)|^2\right]} \qquad (3.7) \\ &= E\left[|Y_L(\omega_m)|^2\right] + \sum_{\omega_k+\omega_l=\omega_m} b'(\omega_k,\omega_l)^2 \cdot S(\omega_m) \end{aligned}$$

where

$$b'(\omega_k,\omega_l) = \left\{\frac{|B(\omega_k,\omega_l)|^2}{E\left[|Y_L(\omega_k)Y_L(\omega_l)|^2\right]\; E\left[|Y(\omega_m)|^2\right]}\right\}^{\frac{1}{2}} \tag{3.8}$$

The second term of Eq. 3.7 represents the accumulation of energy densities associated with interactions that occur at the frequency $\omega_k+\omega_l$. Note that $E[|Y_L(\omega_k)Y_L(\omega_l)|^2]$ in Eq. 3.7 is unknown in advance; hence we may evaluate $E[|Y(\omega_k)Y(\omega_l)|^2]$ and use it as an initial value in finding $b'(\omega_k,\omega_l)$ by iteration.

For the nonlinear components that occur at the frequency $(\omega_k-\omega_l)$, $B^*(\omega_k,\omega_l)$ in Eq. 3.6 and $B(\omega_k,\omega_l)$ in Eq. 3.7 are replaced by $B^*(\omega_l,\omega_k-\omega_l)$ and $B(\omega_l,\omega_k-\omega_l)$, respectively. Thus, we can write

$$S(\omega_m) = E\left[|Y_L(\omega_m)|^2\right] + \sum_{\omega_k+\omega_l=\omega_m} b'(\omega_l,\omega_k-\omega_l)^2 \cdot S(\omega_m) \tag{3.9}$$

where

$$b'(\omega_l,\omega_k-\omega_l) = \left\{\frac{|B(\omega_l,\omega_k-\omega_l)|^2}{E\left[|Y_L(\omega_k)Y_L(\omega_l)|^2\right]\; E\left[|Y(\omega_m)|^2\right]}\right\}^{\frac{1}{2}} \tag{3.10}$$

Note that the domain of the bispectrum in this case is limited to $(B-B_s)$ illustrated in Figure 3.2.

3.2 Example of Application

As an example of application of the method for separating the spectrum into linear and nonlinear components, we may analyze the wave records shown in Figure 3.3, which are portions of the wave data obtained at various water depths in the ARSLOE Project during storm. A brief description about the ARSLOE project is presented in Appendix B.

The three wave records shown in Figure 3.3 were obtained from locations where mean water depths were 21.4, 10.1, and 2.1 meters, respectively. At Gage No. F710, the deepest of the three, the surface profile was almost identical to that observed in deep water waves. As the water depth decreased from the top record to the bottom, the skewness of the surface elevation increased. At Gage No. D615 with mean water depth 2.1 meters, the wave profile shows a definite excess of high crests and shallow troughs because of the limited water depth, which is a typical feature of a non-Gaussian random process. Table 3.1 summarizes the time, distance from the shoreline, water depth, and statistics computed from the time series of surface elevation at three locations.

In order to identify the nonlinear components of waves, bispectrum and bicoherence spectrum are obtained from the time histories at Gage Nos. D615, D625, and F710. The computation of the bispectrum and bicoherence spectrum using Fast Fourier Transform is straightforward. However, care must be taken in estimating the statistical error within a certain significant level. Statistical stability of bispectral estimates is obtained by the ensemble averaging or frequency merging technique. The detailed computational procedure of the bispectral estimation is described in Appendix C.

To understand the nonlinearity of random waves, the bicoherence squared spectrum is used to identify significant triad wave-wave interactions. Figure 3.4 shows the bicoherence spectra at Gage Nos. D615, D625, and F710. To facilitate visualizing the bicoherence plots, only the bicoherence squared values above the 80 percent significance level for zero true bicoherence are shown in the bifrequency octant (see Appendix C for the significance level for zero true bicoherence). The slab thickness of 0.09 in Figure 3.4 indicates the 80 percent

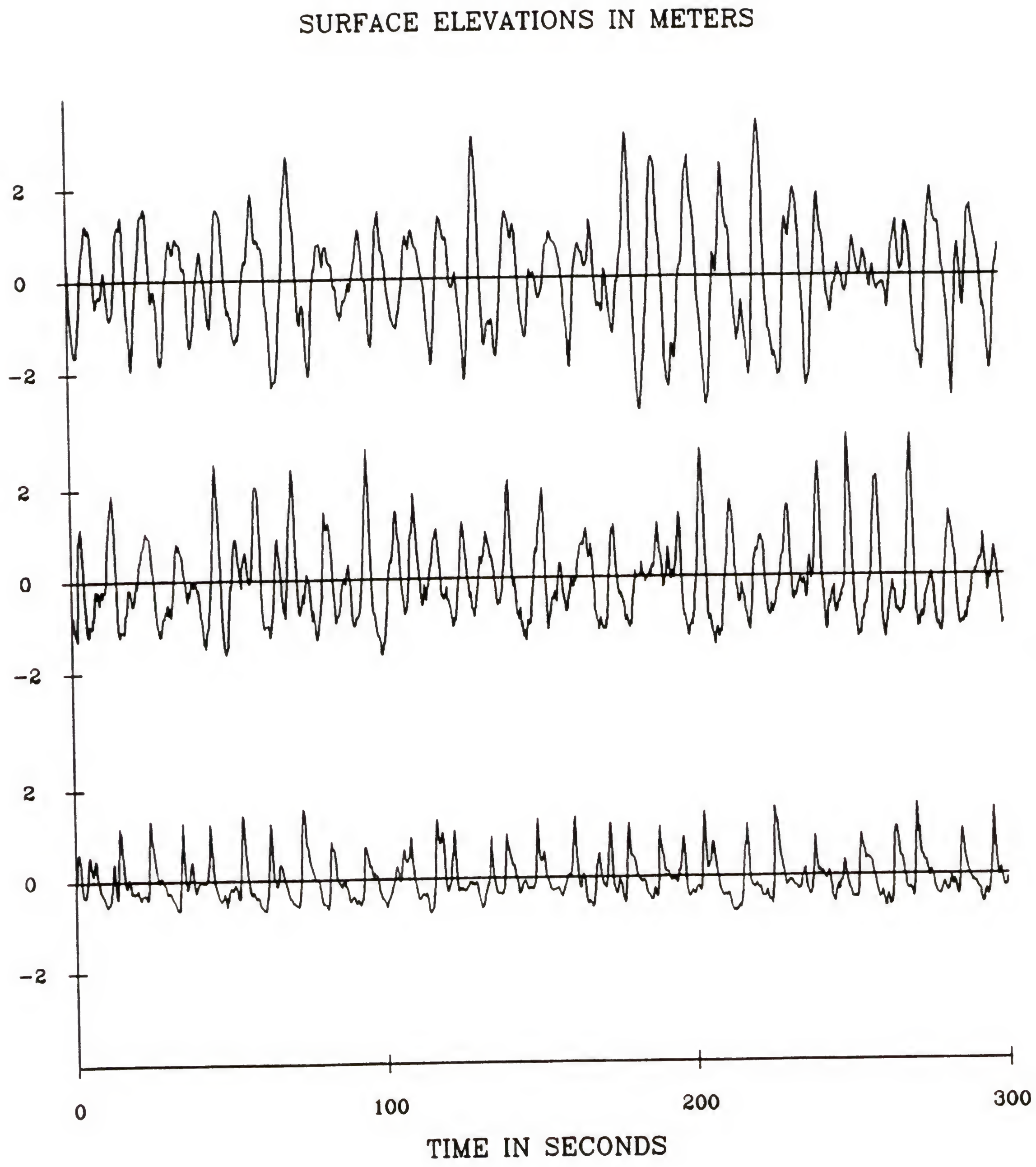

Figure 3.3: Portions of wave records measured during the ARSLOE project at locations F710, D625, and D615 where mean water depths are 21.4, 10.1, and 2.1 meters, respectively.

Table 3.1: Summary of statistics computed from the time histories of surface elevation obtained at Gage Nos. D615, D625, and F710

Gage No.	D615	D625	F710
Time	10/25/80 11:35:00-11:55:00 a.m.	10/25/80 11:35:00-11:55:00 a.m.	10/25/80 11:15:00-11:35:00 a.m.
Distance from the shoreline in meters	60	456	12,000
Mean water depth in meters	2.1	10.07	21.43
Moments of surface Elevation m_2 m_3 m_4	 0.2167 0.1042 0.1958	 0.8507 0.5997 2.5345	 1.0795 -0.0148 3.6721
Variance λ_3 (skewness) λ_4(kurtosis $-$ 3)	0.2167 1.0327 1.1713	0.8507 0.7643 0.5020	1.0795 -0.0132 0.1511
Max. and Min. surface elevation in meters y_{max} y_{min}	 2.25 -1.02	 4.04 -2.19	 3.48 -3.61

significant level for zero bicoherence squared. The frequency resolution $\Delta\omega$ is $2\pi \times 0.0078$ rps, therefore, values in the k and l axes of bifrequency plane in Figure 3.4 multiplied by $\Delta\omega$ are radian frequencies ω_k and ω_l, respectively. The value of minimum density ω_s, defined in Figure 3.1, is assumed to be $7\Delta\omega$ rps at Gage Nos. D615, D625, and F710. At Gage No. F710 in Figure 3.4, two groups of peaks are observed in domains B_s and $(B - B_s)$ as illustrated in Figure 3.2, which indicate sum and difference wave-wave interactions, respectively. For example, a peak located in the bifrequency plane B_s at frequences ω_k and ω_l represents a triad sum interaction, $\omega_k + \omega_l \rightarrow \omega_m$; meaning that the sum interaction between the spectral wave components at ω_k and ω_l generates a new spectral component at ω_m. Furthermore, the bicoherence squared value $b^2(\omega_k,\omega_l)$ represents a fraction of nonlinear energy at ω_m due to spectral components at ω_k and ω_l. Likewise, a peak located in the bifrequency plane $(B - B_s)$ at frequencies ω_l and $(\omega_k - \omega_l)$ represents a triad difference interaction, $\omega_k - \omega_l \rightarrow \omega_m$. As can be seen in Figure 3.4, the number of wave-wave interactions increases dramatically as the water depth decreases.

The bicoherence spectrum can be used for discrimination between nonlinearly coupled components and linear components and for evaluating the fraction of wave energy in a measured spectrum. However, it does not provide any direct information on the relative contribution of the interactions to the total skewness. This information is obtained from the real part of the bispectrum. Figure 3.5 shows the real part of the bispectrum for the same Gage Nos. as Figure 3.4. It is well known that the volume of the real part of the bispectrum represents the mean cube of the record. The real part of the bispectrum $B(\omega_k,\omega_l)$ represents the contribution to the mean cube of the record from the product of three Fourier components whose resultant frequency is zero $(\omega_k + \omega_l + \omega_m = 0)$. For example, Figure 3.5 shows a large peak located around $B(\omega_k,\omega_l) = B(12\Delta\omega, 12\Delta\omega)$, this peak indicates that the self-interaction of primary components at $12\Delta\omega$ generates the first harmonic frequency at $24\Delta\omega$ in the auto spectrum. In order to identify the location of large peaks in the real part of the bispectrum, a contour plot of the bispectrum at Gage No.

D615 is shown in Figure 3.6. The figure indicates that the second largest peak is located at $(\omega_k, \omega_l) = (24\Delta\omega, 12\Delta\omega)$. This interaction indicates that the wave-wave interaction between the primary and the first harmonic components generates a second harmonic component at $36\Delta\omega$ in the auto spectrum.

Figures 3.7, 3.8, and 3.9 show the result of the separation of linear and nonlinear energy spectra obtained at Gage Nos. F710, D625, and D615, respectively. These figures show the ratio of nonlinear energy to the total energy increases as water depth decreases. As is shown in Figure 3.7, almost no energy exists in low frequency components (frequencies less than $\omega_s = 7\Delta\omega = 0.343 \quad rps$). However, Figures 3.8 and 3.9 show that nonlinear components of the spectral density are pronounced at low and high frequencies and that no nonlinear component exists in the neighborhood of the frequency where the spectrum peaks.

The results of this part of the study will be used for the development of a probability density function applicable to the surface elevation of random waves in finite water depth. (See section 4.1 Eq. 4.3.)

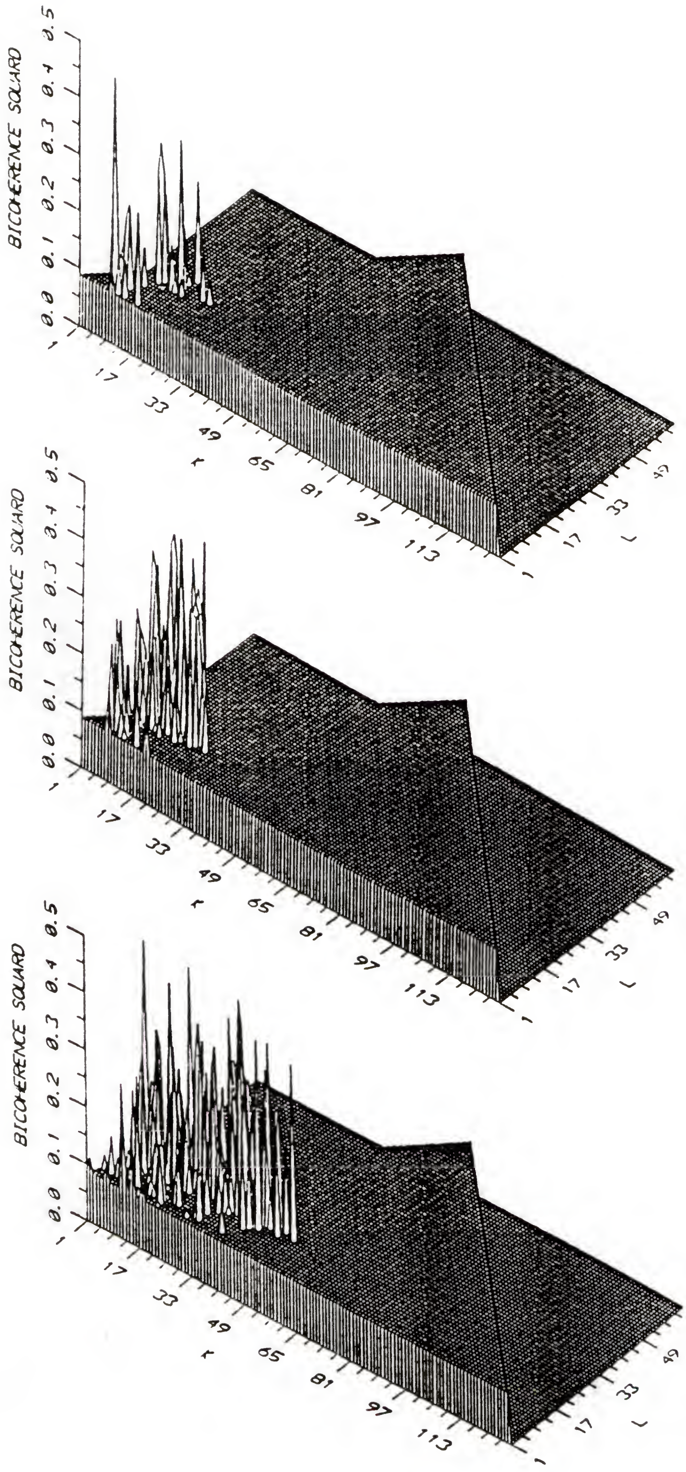

Figure 3.4: Bicoherence squared spectra at Gage Nos. F710, D625, and D615 with water depths of 21.4, 10.1, 2.1 meters, respectively.

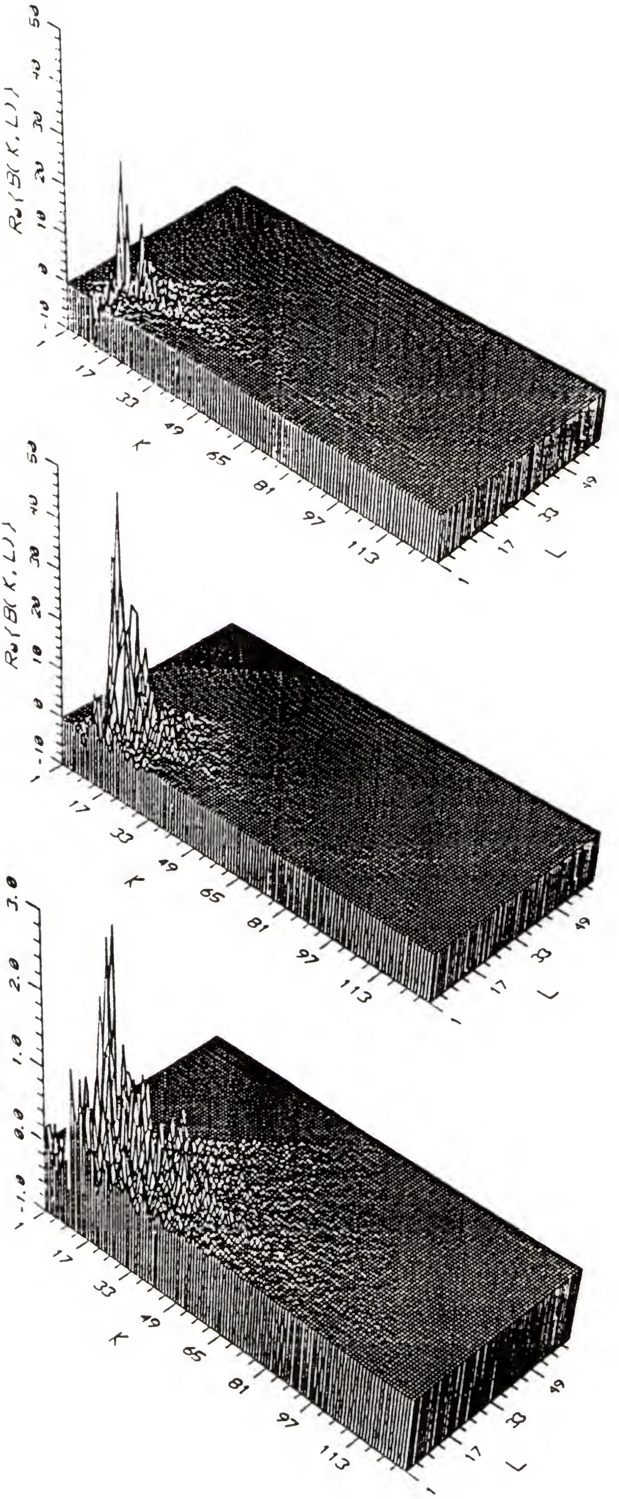

Figure 3.5: Real part of bispectra at Gage Nos. F710, D625, and D615 with water depths of 21.4, 10.1, 2.1 meters, respectively.

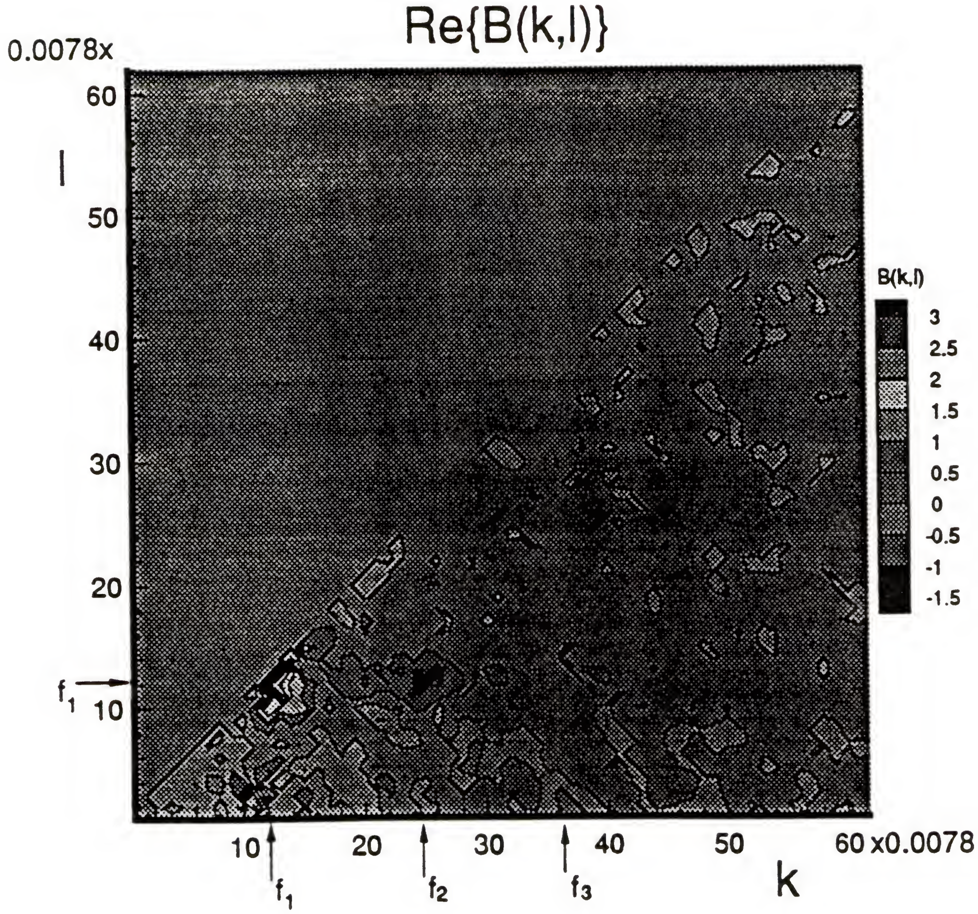

Figure 3.6: Contour plot of the real part of bispectrum at Gage No. D615

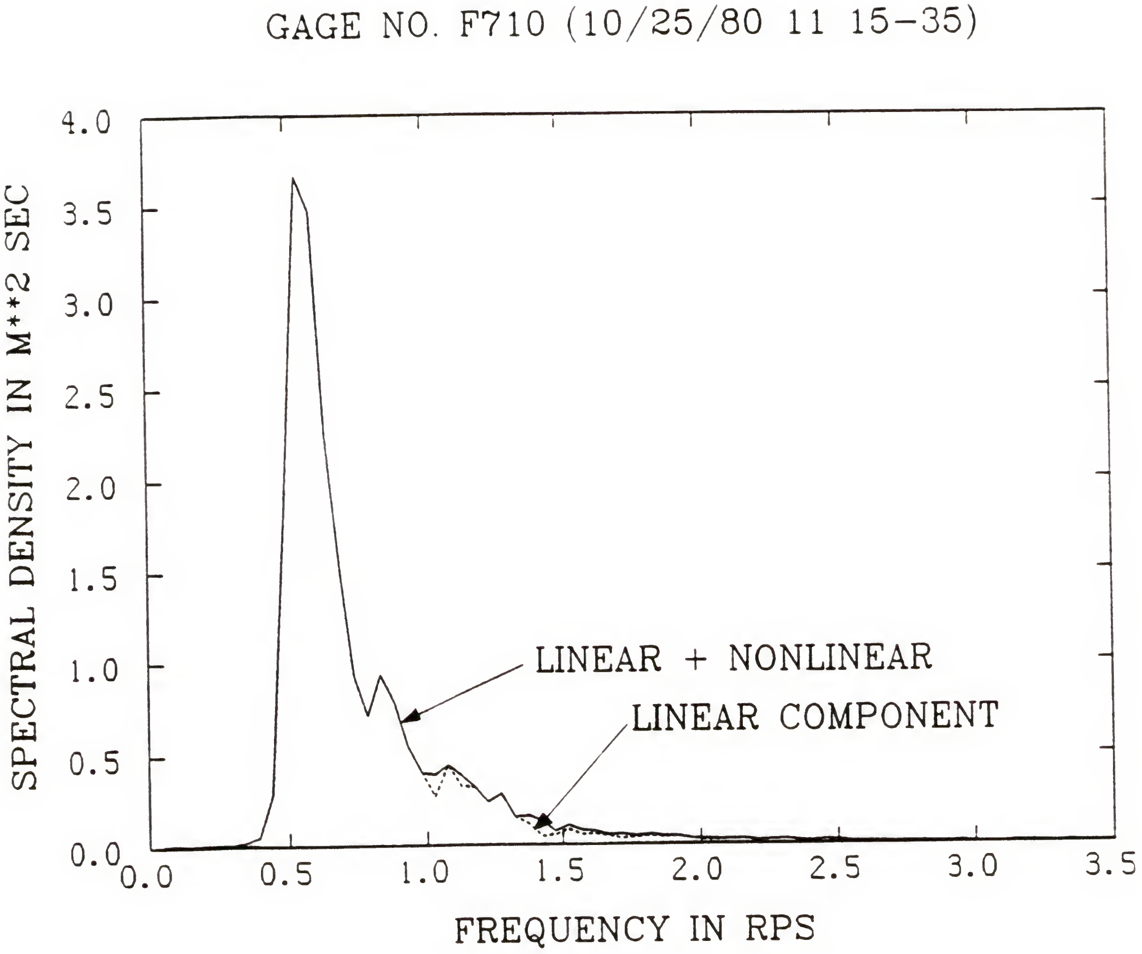

Figure 3.7: Separation of linear and nonlinear components of spectrum at Gage No. F710

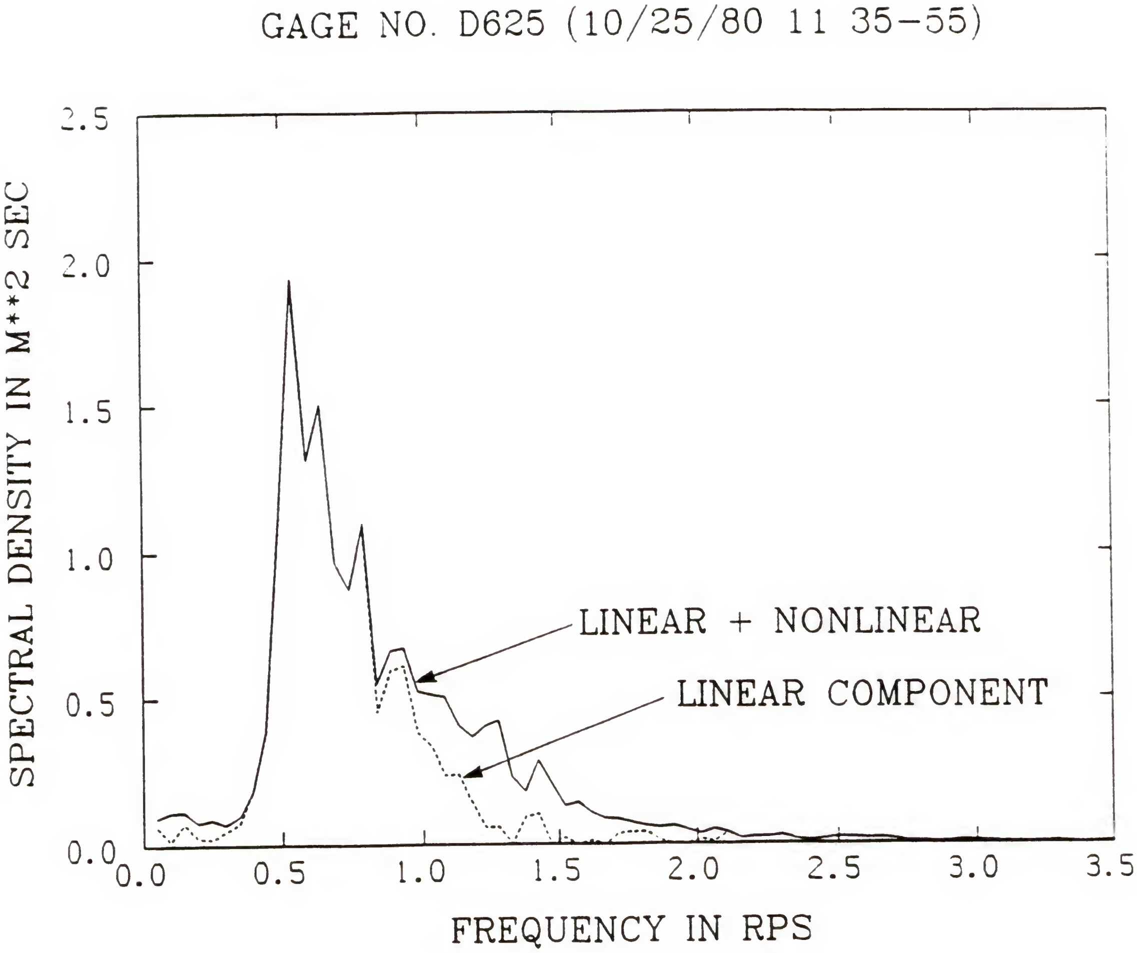

Figure 3.8: Separation of linear and nonlinear components of spectrum at Gage No. D625

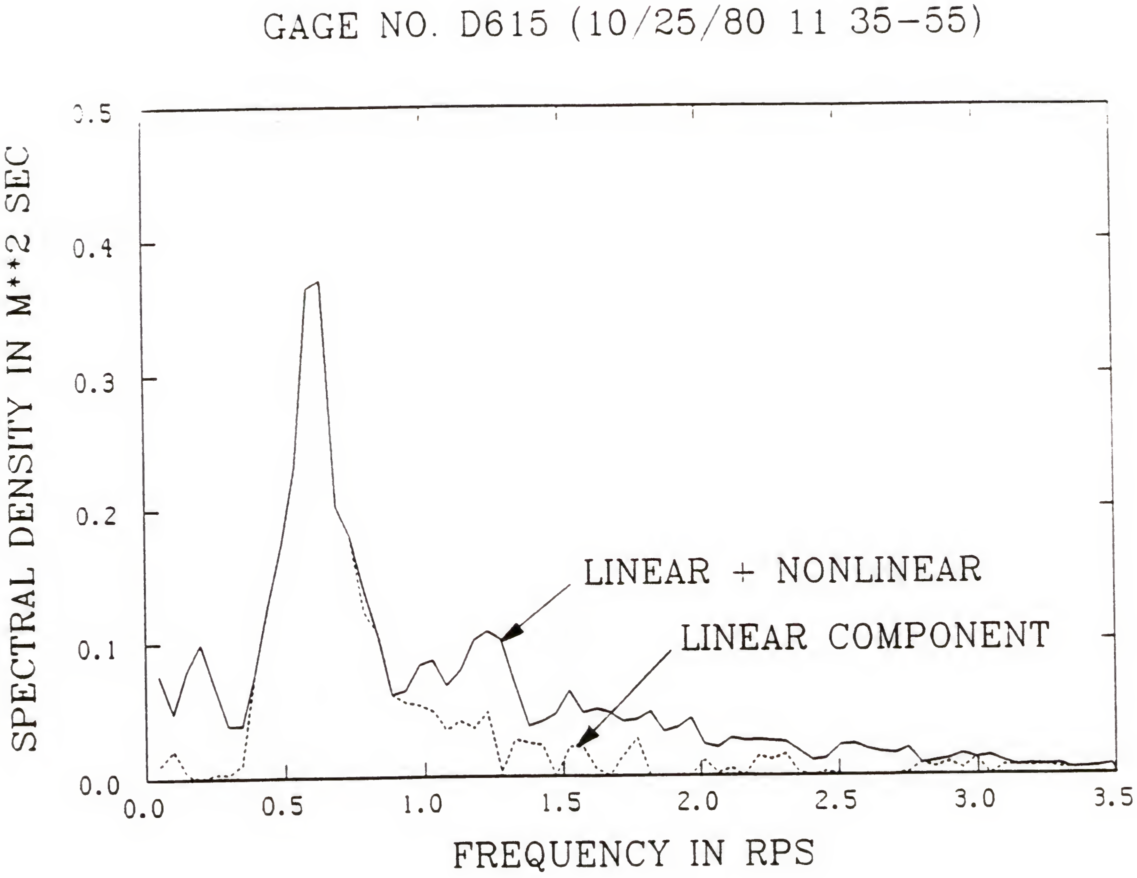

Figure 3.9: Separation of linear and nonlinear components of spectrum at Gage No. D615

CHAPTER 4
PROBABILITY DISTRIBUTION OF WAVE PROFILES

This chapter consists of three sections. In the first section, the application of the concept of Kac-Siegert's method to the probability distribution of waves in finite water depth is discussed. The second-order interaction coefficients are evaluated in terms of bispectral and linear spectral density functions. Numerically computed probability density function and the histogram constructed from the wave data is compared.

In the second section, the derivation of an asymptotic probability density function in closed form is presented by approximating the Kac-Siegert solution as a function of a single random variable whose parameters are determined from information on cumulants k_2 and k_3 of the wave record.

The third section comprises comparisons between the newly developed function and field data obtained in the ARSLOE project during storm for water depths of 2.1, 10.07, and 21.43 meters.

4.1 Application of the Kac-Siegert Method to Probability Distribution of Nonlinear Waves

As stated in Chapter 1, the concept of the Kac-Siegert method is applied for representing the statistical properties of nonlinear waves. For this, we first write the surface profile of second-order random waves in finite water depth as follows:

$$\begin{aligned} y(t) &= Re\sum_{k=1}^{N} c_k\, e^{i(\omega_k\, t+\epsilon_k)} \\ &+ Re\sum_{k=1}^{N}\sum_{l=1}^{N} c_k c_l \left[q_{kl}\, e^{\{(\omega_k+\omega_l)t+(\epsilon_k+\epsilon_l)\}} + r_{kl}\, e^{\{(\omega_k-\omega_l)t+(\epsilon_k-\epsilon_l)\}}\right] \end{aligned} \tag{4.1}$$

where ω = radian frequency, ϵ = phase lag.

q_{kl} is a coefficient associated with $(\omega_k + \omega_l)$, which is the sum of the interaction between two frequency components ω_k and ω_l, while r_{kl} is associated with the difference of the interaction between ω_k and ω_l. Since there is a phase shift between the two frequencies ω_k and ω_l, in general, these interaction coefficients are complex numbers.

As reviewed in Chapter 2, Eq. 4.1 has often been considered for analysis of nonlinear random waves in which the interaction coefficients are evaluated from the weakly nonlinear solution. However, the weakly nonlinear solution cannot be applied to the present problem. Instead, we will obtain the interaction coefficients through spectral analysis. For this, let us write the first term of Eq. 4.1 as follows:

$$\sum_{k=1}^{N} c_k e^{i(\omega_k t + \epsilon_k)} = \sum_{k=1}^{N} c_k \{\cos(\omega_k t + \epsilon_k) + i\ \sin(\omega_k t + \epsilon_k)\} \tag{4.2}$$

We assume that the linear component $y_1(t)$ is a Gaussian random process. By ignoring the factor ρg, $\frac{1}{2}c_k^2$ represents the spectral density denoted by $2S_L(\omega_k)\Delta\omega$, where the subscript L stands for the spectral density associated with the linear wave components. That is, the spectral density at $\omega = \omega_k$ is written by

$$s_k = \{2S_L(\omega_k)\Delta\omega\}^{1/2} = \left\{\int_{\omega_k - \frac{\Delta\omega}{2}}^{\omega_k + \frac{\Delta\omega}{2}} 2S_L(\omega)d\omega\right\}^{\frac{1}{2}} \tag{4.3}$$

Then by defining

$$\begin{aligned} c_k \ \ \cos(\omega_k t + \epsilon_k) &= s_k\, u_k \\ c_k \ \ \sin(\omega_k t + \epsilon_k) &= s_k\, v_k \end{aligned} \tag{4.4}$$

Eq. 4.2 can be written as

$$y_1(t) = Re \sum_{k=1}^{N} s_k(u_k + i\, v_k) \tag{4.5}$$

Note that the left side of Eq. 4.4 is associated with a Gaussian distribution with zero mean and variance s_k^2; hence, u_k and v_k are statistically independent random variables.

Similarly, the second term of Eq. 4.1 can be written as

$$y_2(t) = Re \sum_{k=1}^{N}\sum_{l=1}^{N} s_k\, s_l\, \{\, q_{kl}\, (u_k + i\, v_k)(u_l + i\, v_l) + r_{kl}(u_k + i\, v_k)(u_l - i\, v_l)\,\} \tag{4.6}$$

where

$$s_l = \{2S_L(\omega_l)\Delta\omega\}^{\frac{1}{2}}. \tag{4.7}$$

By taking the real-part of Eq. 4.5 and 4.6, we have

$$\begin{aligned} y(t) &= y_1(t) + y_2(t) \\ &= \sum_{k=1}^{N} s_k u_k + \sum_{k=1}^{N}\sum_{l=1}^{N}\{s_k s_l(q_{kl}+r_{kl})u_k u_l + s_k s_l(q_{kl}-r_{kl})v_k v_l\} \end{aligned} \tag{4.8}$$

To evaluate s_k and s_l in Eq. 4.8, it is necessary to separate the auto spectrum of waves into two parts; one associated with linear components, the other associated with nonlinear components of the waves. The method of separation of linear components from the auto spectrum is presented in the previous chapter. The interaction coefficients q_{kl} and r_{kl} in Eq. 4.8 will be obtained with the aid of the bispectrum of the waves $y(t)$.

Let us consider the bispectrum $B(\omega_k, \omega_l)$. The bispectrum is most commonly evaluated in the fundamental region, which is the octant, the domain defined by $0 \le \omega_l \le \omega_k$ and $0 \le \omega_k \le \infty$ as shown in Figure 3.2. The volume under the bispectrum is equal to the 3rd moment of $y(t)$ when the mean value of $y(t)$ is zero. That is, the 3rd moment is given by

$$E\left[\{y(t)\}^3\right] = 6\sum_{k=1}^{N}\sum_{l=1}^{N} Re\{B(\omega_k, \omega_l)\} \tag{4.9}$$

On the other hand, the third moment of $y(t) = y_1(t) + y_2(t)$ can be obtained as

$$E\left[\{y(t)\}^3\right] = 3E\left[y_1(t)^2 y_2(t)\right] + E\left[\{y_2(t)\}^3\right] \tag{4.10}$$

Note that since $y_1(t)$ is a normal distribution with zero mean, that $E[\{y_1(t)\}^3]$ and $E[y_1(t)\{y_2(t)\}^2]$ are zero.

The linear component $y_1(t)$ is usually much greater than the nonlinear component $y_2(t)$; therefore, the second term of Eq. 4.10 may be neglected in comparison with the first term. Hence, we have from Eq. 4.8,

$$E\left[\{y(t)\}^3\right] = 3E\left[y_1(t)^2 y_2(t)\right] = 6\sum_{k=1}^{N}\sum_{l=1}^{N} s_k^2 s_l^2 (q_{kl} + r_{kl}) \tag{4.11}$$

Then, Eqs. 4.9 and 4.11 yield

$$\sum_{k=1}^{N}\sum_{l=1}^{N}(q_{kl}+r_{kl})=\sum_{k=1}^{N}\sum_{l=1}^{N}\frac{Re\{B(\omega_k,\omega_l)\}}{s_k^2 s_l^2} \tag{4.12}$$

As stated in the previous section, the domain of the spectrum applicable for the interactions associated with the sum of two frequency components is B_s shown in Figure 3.2. Therefore, from Eq. 4.12, the interaction coefficient q_{kl} can be obtained as

$$q_{kl}=\frac{1}{s_k^2 s_l^2}B_s(\omega_k,\omega_l) \tag{4.13}$$

Similarly, the interaction coefficient r_{kl} can be evaluated as

$$r_{kl}=\frac{1}{s_k^2 s_l^2}\{B(\omega_l,\omega_k-\omega_l)-B_s(\omega_k,\omega_l)\} \tag{4.14}$$

The functional relationship between the interaction coefficients q_{kl}, r_{kl} and the parameters β_j and λ_j of Kac-Siegert's solution was derived in matrix form by Langley (1987). Although Langley obtained the interaction coefficients from the potential theory, the functional relationship between (q_{kl}, r_{kl}) and (β_j, λ_j) can still be applied to the present problem. Langley presented Eq. 4.8 in the following matrix form:

$$y(t)=\underline{s}^T\,\underline{u}+\underline{u}^T(\underline{Q}+\underline{R})\,\underline{u}+\underline{v}^T(\underline{Q}-\underline{R})\,\underline{v} \tag{4.15}$$

where $\underline{Q}$ and $\underline{R}$ are real symmetric matrices whose kl-th components are $s_k s_l q_{kl}$ and $s_k s_l r_{kl}$, and $\underline{s}$, $\underline{u}$, and $\underline{v}$ are vectors whose kl-th components are s_k, u_k, and v_k, respectively. We may write two matrices in Eq. 4.15 as

$$\begin{aligned}\underline{Q}+\underline{R} &= \underline{w}_1^T\Lambda_1\underline{w}_1 \\ \underline{Q}-\underline{R} &= \underline{w}_2^T\Lambda_2\underline{w}_2\end{aligned} \tag{4.16}$$

where the column vectors of $\underline{w}_j$ $(j=1,2)$ are normalized eigenvectors. They are orthonormal vectors satisfying the condition $\underline{w}_j^T\cdot\underline{w}_j=\underline{I}$, where $\underline{I}$ is the identity matrix. The elements of diagonal matrices $\underline{\Lambda}_j$ $(j=1,2)$ are eigenvalues of matrix $\underline{Q}+\underline{R}$ and $\underline{Q}-\underline{R}$, respectively. Since $\underline{Q}+\underline{R}$ and $\underline{Q}-\underline{R}$ are N by N symmetric matrices, there are a total of $2N$ eigenvalues.

Futhermore, by writing

$$Z_j = \begin{cases} (\underline{w}_1^T \underline{u})_j, & j = 1, 2, \cdots N \\ (\underline{w}_2^T \underline{v})_{j-N}, & j = (N+1), \cdots 2N \end{cases} \tag{4.17}$$

where Z_j is an independent Gaussian random variable with zero mean and unit variance, Langley has shown that Eq. 4.15 can be reduced to the Kac-Siegert's formulation given in Appendix A Eq. A.2 with the following relationships:

$$\beta_j = \begin{cases} (\underline{s}^T \underline{w}_1)_j, & j = 1, 2, \cdots N \\ 0, & j = (N+1), \cdots 2N \end{cases} \tag{4.18}$$

$$\lambda_j = \begin{cases} (\underline{\Lambda}_1)_j & j = 1, 2, \cdots N \\ (\underline{\Lambda}_2)_j, & j = (N+1), \cdots 2N \end{cases} \tag{4.19}$$

By employing the parameters β_j and λ_j obtained in Eqs. 4.18 and 4.19, the probability density function of $y(t)$ can be derived numerically from Eq. A.2. Hereafter, $y(t)$ will be written as a random variable Y. The most convenient way to derive the probability density function is through the characteristic function as suggested by Kac and Siegert. That is, the characteristic function of Eq. A.2 is given by

$$\phi(t) = \prod_{j=1}^{2N} (1 - i2\lambda_j t)^{-\frac{1}{2}} \cdot \exp\left\{ -\sum_{j=1}^{2N} \frac{\beta_j^2 t^2}{2(1 - i2\lambda_j t)} \right\} \tag{4.20}$$

and therefrom the probability density function of Y can be numerically derived by

$$f(y) = \frac{1}{2\pi} \int_{-\infty}^{\infty} \phi(t)\ e^{-ity}\, dt \tag{4.21}$$

The method stated above is applied to the data obtained at Gage No. D615 shown in Figure 3.3 in which β_j and λ_j are evaluated by Eqs. 4.18 and 4.19 for $N = 128$ points. A comparison between the probability density function and the histogram constructed from the data is shown in Figure 4.1. Excellent agreement between them can be seen in the figure.

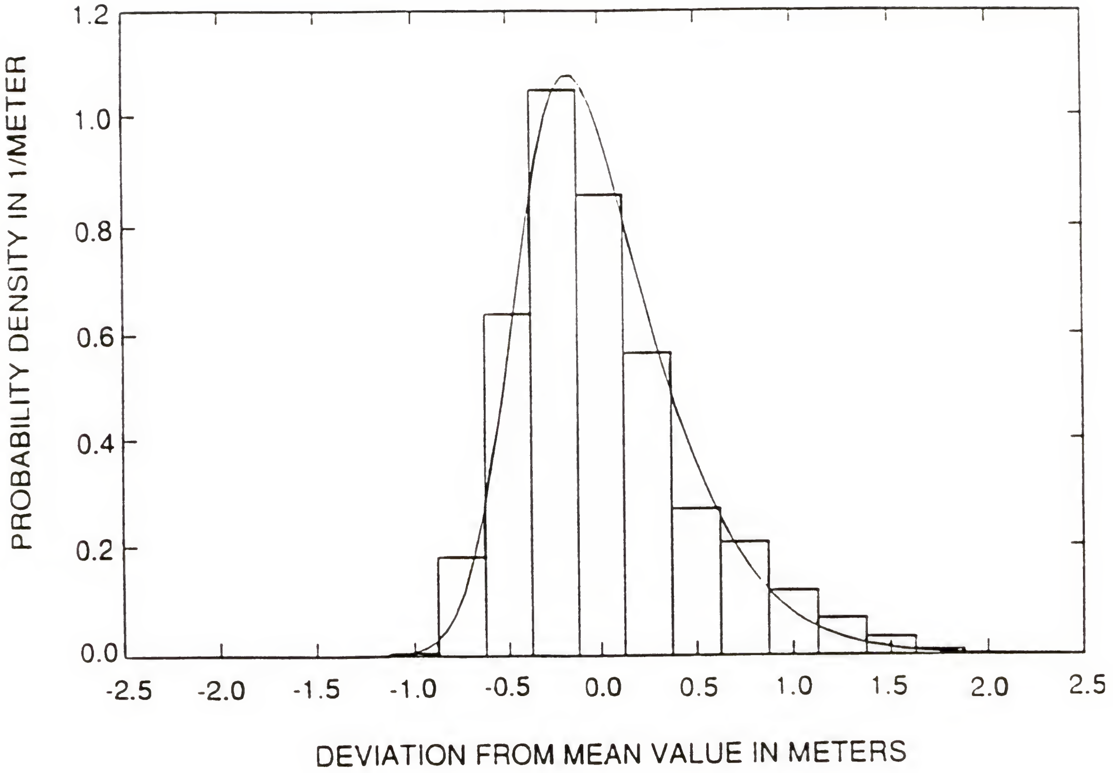

Figure 4.1: Comparison of probability density function obtained from Kac-Siegert's solution and histogram constructed from data

4.2 Derivation of Asymptotic Probability Density Function

As demonstrated in the previous section, Kac-Siegert's solution satisfactorily yields a probability density function applicable to nonlinear random waves in finite water depth. The probability density function, however, is not given in closed form. One way to derive the probability density function in closed form is to present Kac-Siegert's solution (Eq. A.2) as a function of a single random variable instead of the summation of the standardized normal distribution and its squared quantity. For this, let us present Eq. A.2 as

$$Y = U + aU^2 \tag{4.22}$$

where "a" is a constant (unknown) and U is a normal variate with mean μ_* and variance σ_*^2, both of which are also unknown. The value of these unknowns will be determined by equating the characteristic function of Eq. 4.22 with that of Kac-Siegert's solution given in Eq. 4.20.

In order to obtain the characteristic function of Eq. 4.22, let us write

$$Y = \left\{\sqrt{a}\left(U + \frac{1}{2a}\right)\right\}^2 - \frac{1}{4a} = U_0^2 - \frac{1}{4a} \tag{4.23}$$

where

$$U_0 = \sqrt{a}\left(U + \frac{1}{2a}\right) . \tag{4.24}$$

Since U is a normal variate with mean μ_* and variance σ_*^2, U_0 follows the normal distribution with mean $\sqrt{a}\sigma_* + (1/(2\sqrt{a}))$ and variance $a\sigma_*^2$. Therefore, the characteristic function of U_0^2 becomes

$$\phi(t) = \frac{1}{\sqrt{1 - i2a\sigma_*^2 t}} \exp\left\{\frac{it\left(\sqrt{a}\mu_* + \frac{1}{2\sqrt{a}}\right)^2}{1 - i2a\sigma_*^2 t}\right\} \tag{4.25}$$

The characteristic function of the second term of Eq. 4.23 is given by

$$\phi(t) = \exp\left\{-\frac{it}{4a}\right\} \tag{4.26}$$

Thus, the characteristic function of Y is the product of Eqs. 4.25 and 4.26 which after some mathematical manipulation can be written as follows:

$$\phi(t) = \frac{1}{\sqrt{1 - i2a\sigma_*^2 t}} \exp\left\{ \left(a\mu_*^2 + \mu_* + \frac{\sigma_*^2}{2} it \right) \left(\frac{it}{1 - i2a\sigma_*^2 t} \right) \right\} \tag{4.27}$$

By taking the logarithm of the characteristic function and by expanding it in a series of (it), we have

$$\begin{aligned} ln\phi(t) &= (a\sigma_*^2 + a\mu_*^2 + \mu_*)(it) + \left\{ a^2\sigma_*^4 + \frac{\sigma_*^2}{2} 2a\sigma_*^2(a\mu_*^2 + \mu_*) \right\} (it)^2 \\ &+ \left\{ \frac{4}{3} a^3\sigma_*^6 + a\sigma_*^4 + 4a^2\sigma_*^4(a\mu_*^2 + \mu_*) \right\} (it)^3 + \cdots \end{aligned} \tag{4.28}$$

On the other hand, by taking the logarithm of the characteristic function of Kac-Siegert's solution (Eq. A.2), and by expanding it in a series of (it), we have

$$\begin{aligned} ln\phi(t) &= \left(\sum_{j=1}^{2N} \lambda_j \right) (it) + \left(\frac{1}{2} \sum_{j=1}^{2N} \beta_j^2 + \sum_{j=1}^{2N} \lambda_j^2 \right) (it)^2 \\ &+ \left(\sum_{j=1}^{2N} \beta_j^2 \lambda_j + \frac{4}{3} \sum_{j=1}^{2N} \lambda_j^3 \right) (it)^3 + \cdots \end{aligned} \tag{4.29}$$

Note that the first term is $\sum \lambda_j = 0$, since the mean value of Y is zero. Comparing Eqs. 4.28 and 4.29, the following relationship can be derived:

$$\left\{ \begin{aligned} & a\sigma_*^2 + a\mu_*^2 + \mu_* = 0 \\ & \sum_{j=1}^{2N} \beta^2 + 2\sum_{j=1}^{2N} \lambda_j^2 = \sigma_*^2 - 2a^2\sigma_*^4 \\ & 3\sum_{j=1}^{2N} \beta_j^2 \lambda_j + 4\sum_{j=1}^{2N} \lambda_j^3 = 3a\sigma_*^4 - 8a^3\sigma_*^6 \end{aligned} \right. \tag{4.30}$$

By using the values of β_j and λ_j evaluated in the previous section, we can determine the unknown parameters a, μ_*, and σ_*^2 from Eq. 4.30. Since U in Eq. 4.22 is now a normal variate with known mean and variance, the probability density function of Y can be derived by applying the technique of change of random variables from U to Y. The density function can be obtained as

$$\begin{aligned} f(y) &= \frac{1}{\sqrt{2\pi}a\sigma_*}\frac{1}{\sqrt{y+\frac{1}{4a}}} \\ &\times \; \exp\left\{-\left[y+\left(\sqrt{a}\mu_*+\frac{1}{2\sqrt{a}}\right)^2+\frac{1}{4a}\right]/(2a\sigma_*^2)\right\} \\ &\times \; \cosh\left\{\left(\sqrt{a}\mu_*+\frac{1}{2\sqrt{a}}\right)\sqrt{y+\frac{1}{4a}}/(a\sigma_*^2)\right\} \end{aligned} \tag{4.31}$$

A comparison of the asymptotic probability density function shown in Eq. 4.31 and that obtained numerically from the characteristic function of Kac-Siegert's solution is shown in Figure 4.2 along with the histogram of a random process. As can be seen in the figure, the asymptotic probability density function agrees well with that obtained from the Kac-Siegert solution. Unfortunately, however, the density function vanishes at the point $y = -(1/4a)$ due to a singular point involved in the density function. Because of this drawback, Eq. 4.31 cannot be considered as an appropriate density function.

Next, let us present the functional relationship between Y and U given in Eq. 4.22 inversely such that the random variable U is expressed as a function of Y as follows:

$$U = \frac{1}{\gamma a}\left(1 - e^{\gamma a Y}\right) \tag{4.32}$$

where γ is a constant; 1.28 for $y \geq 0$ and 3.00 for $y \leq 0$. Justification for selecting these constant values of γ is given in Appendix D. It may suffice here to say that these constants are determined from dimensionless quantities of Y and U, and that the constants are valid even for waves with very strong nonlinear characteristics.

It is noted that the values of γ are different for positive and negative y-values. This results in a slight difference in the slope of the probability density function at $y = 0$, although the density function is continuous at this point.

Figure 4.3 shows a comparison of Eq. 4.22 and Eq. 4.32 for $a = 0.326$. The a-value is obtained from Eq. 4.30 for the non-Gaussian random process shown in Figure 3.3, Gage No. D615 which has a very large skewness, 1.03. The random process may be considered as if it

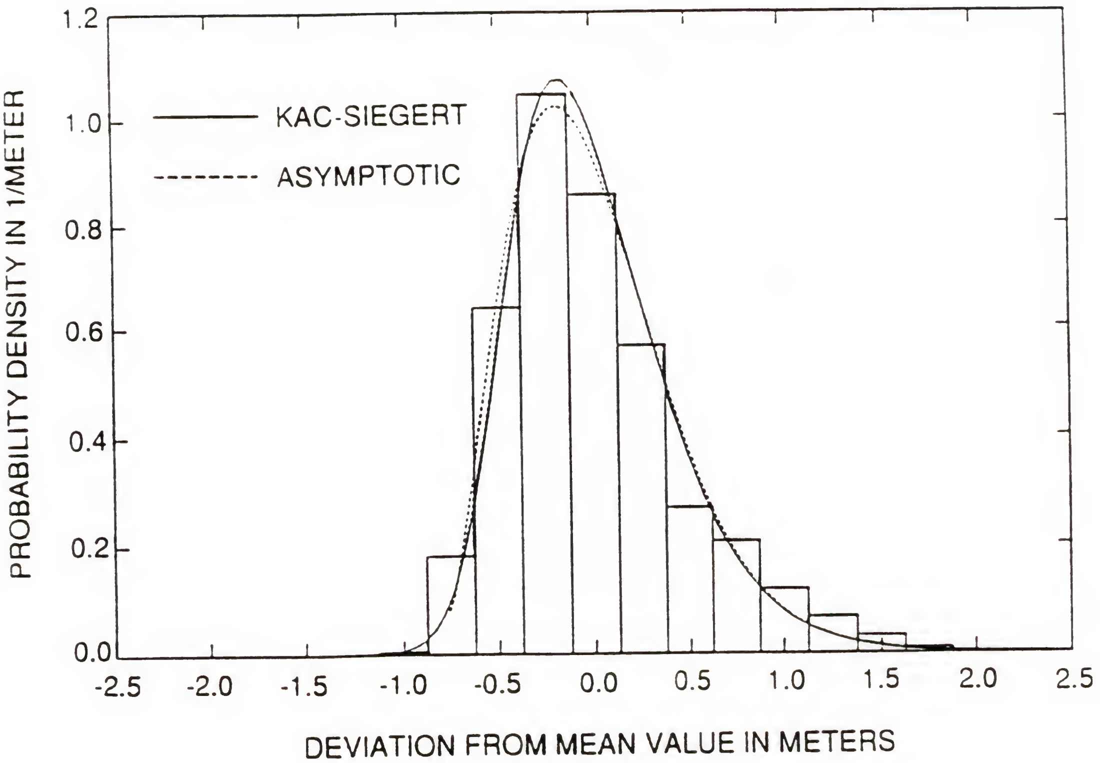

Figure 4.2: Comparison between Kac-Siegert and asymptotic probability density functions and histogram constructed from data

were random waves with very severe nonlinearity. As can be seen in the figure, Eq. 4.32 well represents Eq. 4.22 except in the negative range of y where Eq. 4.22 has a singular point.

By using the functional relationship given in Eq. 4.32, we may derive the probability density function of Y from the random variable U which obeys the normal distribution with mean μ_* and variance σ_*^2. The change of random variable technique yields the probability density function of Y as follows:

$$f(y) = \frac{1}{\sqrt{2\pi}\sigma_*} \exp\left\{ -\frac{1}{2(\gamma a \sigma_*)^2} \left(1 - \gamma a \mu_* - e^{-\gamma a y}\right)^2 - \gamma a y \right\} \tag{4.33}$$

where

$$\gamma = \begin{cases} 1.28 & y \geq 0 \\ 3.00 & y < 0. \end{cases} \tag{4.34}$$

By applying the method for determining the limit of an indefinite function, it can be easily proved that Eq. 4.33 reduces to a normal probability density function with mean μ_* and variance σ_*^2 if $a = 0$; namely, for linear random waves.

It was stated earlier that a, μ_*, and σ_*^2 are determined from Eq. 4.30 using β_j and λ_j values of Kac-Siegert's solution. However, this method of evaluating a, μ_*, and σ_*^2 can be greatly simplified if we consider the cumulants of the distribution. That is, the cumulant generating function, denoted by $\psi(t)$, of the Kac-Siegert solution can be obtained from Eq. 4.20 as follows:

$$\psi(t) = ln\phi(t) = -\frac{1}{2}\sum_{j=1}^{2N} ln(1 - i2\lambda_j t) - \sum_{j=1}^{2N} \frac{\beta_j t^2}{2} \frac{1}{1 - i2\lambda_j t} \tag{4.35}$$

By expanding the first and second terms in a series of (it), we have

$$\begin{aligned} \psi(t) &= \left(\sum_{j=1}^{2N} \lambda_j\right)(it) + \frac{1}{2!}\left(\sum_{j=1}^{2N} \beta_j^2 + 2\sum_{j=1}^{2N} \lambda_j^2\right)(it)^2 \\ &+ \frac{1}{3!}\left(6\sum_{j=1}^{2N} \beta_j^2 \lambda_j + 8\sum_{j=1}^{2N} \lambda_j^3\right)(it)^3 + \cdots \end{aligned} \tag{4.36}$$

On the other hand, the cumulant generating function can be written in terms of cumu-

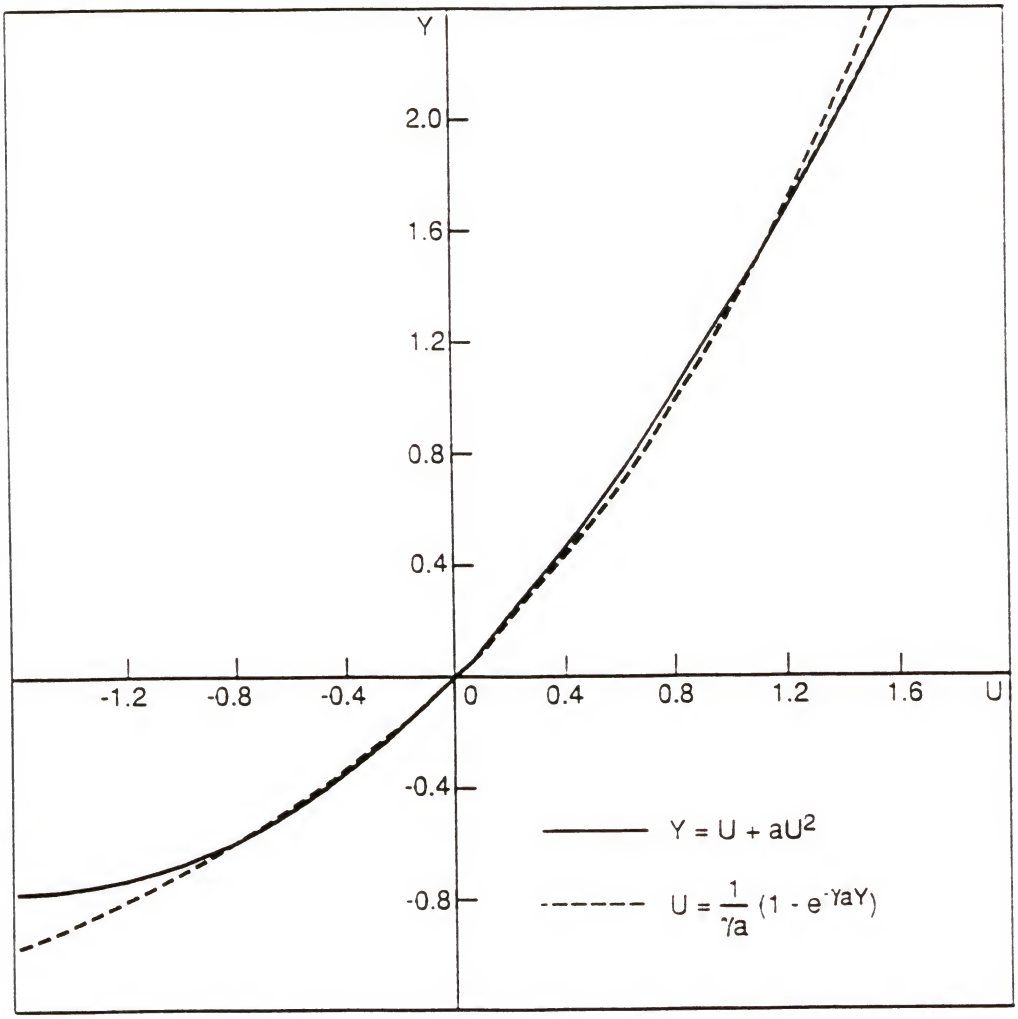

Figure 4.3: Comparison of $Y = U + aU^2$ and $U = (1 - \exp\{-a\gamma Y\})/\gamma a$ for $a = 0.326$

lants as follows:

$$\psi(t) = \sum_{s=1}^{\infty} k_s \frac{(it)^s}{s!} = k_1(it) + \frac{1}{2!}k_2(it)^2 + \frac{1}{3!}k_3(it)^3 + \cdots \tag{4.37}$$

where $k_s =$ cumulants.

From comparison of Eqs. 4.36 and 4.37, we have the following relationships:

$$\begin{aligned} k_1 &= \sum_{j=1}^{2N} \lambda_j \\ k_2 &= \sum_{j=1}^{2N} \beta_j^2 + 2\sum_{j=1}^{2N} \lambda_j^2 \\ k_3 &= 6\sum_{j=1}^{2N} \beta_j^2 \lambda_j + 8\sum_{j=1}^{2N} \lambda_j^3, \quad \text{etc.} \end{aligned} \tag{4.38}$$

Therefore, Eq. 4.30 can be written as

$$\begin{cases} a\sigma_*^2 + a\mu_*^2 + \mu_* = 0 \\ \sigma_*^2 - 2a^2\sigma_*^4 = k_2 \\ 2a\sigma_*^4(3 - 8a^2\sigma_*^2) = k_3 \end{cases} \tag{4.39}$$

Since the mean value of the surface elevation Y is zero for the present problem, we have $k_1 = 0$, and thereby k_2 and k_3 are equal to the sample moments $E[y^2]$ and $E[y^3]$, respectively. Thus, we can determine the unknown parameters a, μ_*, and σ_*^2 by simply evaluating the sample moments from the wave profile record $y(t)$.

4.3 Application of the Probability Density Function to Field Data

The newly developed probability density function applicable to surface profiles of random waves in finite water depth is compared with the histograms constructed from field data obtained at various water depths. The wave data used are shown in Figure 3.3.

As mentioned in the previous section, the parameters a, μ_*, and σ_*^2 are determined from Eq. 4.39 with the cumulants k_2 and k_3 computed from the record. Table 4.1 shows the parameters computed at three different water depths.

Figures 4.4, 4.5, and 4.6 show comparisons of the probability density function given in Eq. 4.33 and the histogram constructed from wave record at Gage Nos. D615, D625, and

Table 4.1: Parameters computed from the cumulants of surface elevation at Gage Nos. D615, D625, and F710

Gage No.	D615	D625	F710
Cumulants of surface Elevation in meters			
k_2	0.2167	0.8507	1.0795
k_3	0.1042	0.5997	−0.0148
Parameters Computed			
a	0.3716	0.1351	−0.0021
μ_*	−0.089	−0.121	0.002
σ_*^2	0.2315	0.8790	1.0795

F710, respectively. Included also in the figures are the normal probability density function with zero mean and variance evaluated from the records. Figure 4.4 shows a comparison for waves in shallow water areas (mean water depth 2.1 meters). As can be seen, the histogram deviates from the normal density function to a great extent; but the agreement between the histogram and the newly developed probability density function is excellent.

Figure 4.5 shows the case for waves in water depth 10.1 m in which the skewness representing the degree of nonlinearity of waves is less than that of Figure 4.4. Again, the probability density function shows excellent agreement with the histogram.

Figure 4.6 shows a comparison for a water depth of 21.4 m. In this case, the distribution of surface elevation is the normal distribution as shown in the figure because the water depth is relatively deep. The histogram and the newly developed probability density function agree very well in this case.

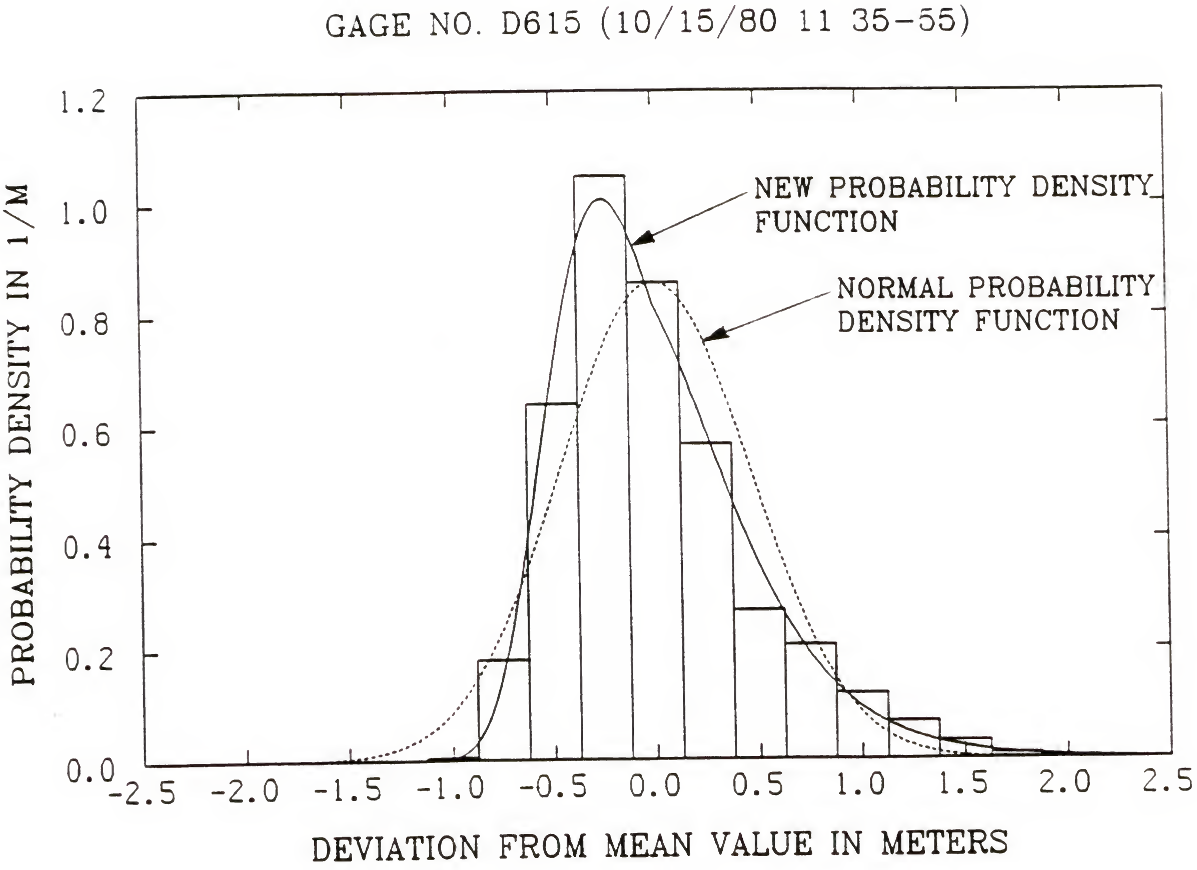

Figure 4.4: Comparison of newly developed probability density function and histogram constructed from data at Gage No. D615

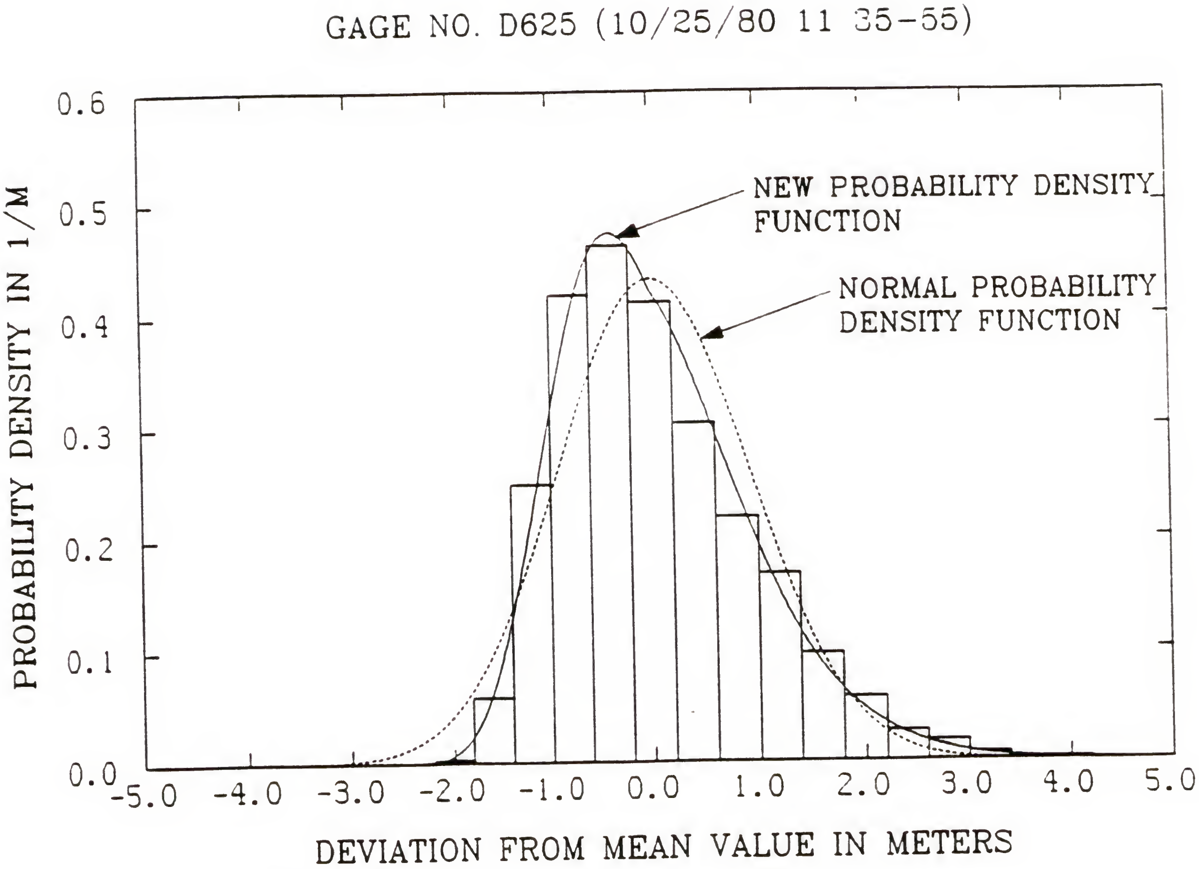

Figure 4.5: Comparison of newly developed probability density function and histogram constructed from data at Gage N0. D625

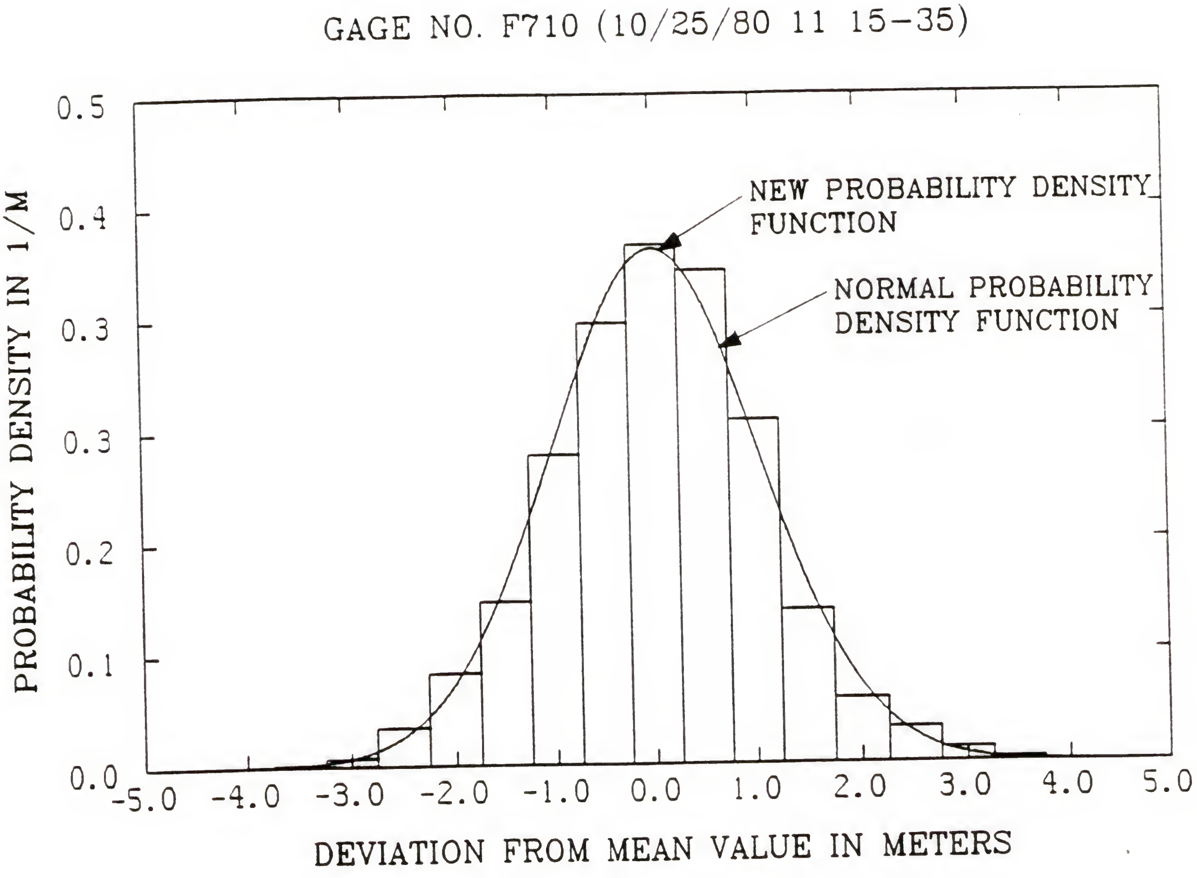

Figure 4.6: Comparison of newly developed probability density function and histogram constructed from data at Gage No. F710

CHAPTER 5
CONCLUSIONS

This paper presents the results of a study on nonlinear analysis of random waves in finite water depth, in particular, this study seeks to (1) clarify nonlinearities in wave spectra, and (2) develop a probability density function in closed form which is applicable to random waves in finite water depth.

In the first phase of the study, a method to separate the second-order spectrum from the measured spectrum was developed. The method employed bicoherence spectrum through which nonlinear characteristics of waves in finite water depth were clarified. The method was applied to field data at different water depths obtained in the ARSLOE Project during storm.

From the results of a separation of the second-order spectrum from the measured spectrum, it was found that no nonlinear components existed near the spectrum peak frequency, ω_p. In shallow water depth, nonlinear components of the spectral density were pronounced at high and low frequencies which indicated that a considerable number of occurrences of wave-wave interactions were associated with various pairs of two frequency components.

It was also found that the ratio of nonlinear energy to the total energy increased with decreasing water depth. This nonlinear energy was associated with mainly self-interactions at frequencies near ω_p. The interactions between frequencies in the neighborhood of ω_p and their harmonic components ($2\omega_p$ or $3\omega_p$) became pronounced with decreasing water depth.

In the second phase of the study, the probability density function applicable to random waves in finite water depth was developed in closed form by applying the concept of Kac-Siegert's method for evaluating the response of a nonlinear mechanical system. That is, the Kac-Siegert formula was expressed in terms of a random variable which obeys a normal distribution with parameters evaluated from information on cumulants of the wave record. Then, by applying the transformation technique of random variables, the probability density function applicable to nonlinear random waves was developed in closed form. Comparisons between the newly developed probability density function and the histograms constructed from wave records at various water depths obtained in the ARSLOE Project during strom showed excellent agreement.

APPENDIX A
KAC-SIEGERT'S METHOD

The response of a nonlinear system is often presented by Volterra's stochastic series expansion given by

$$\begin{aligned} y(t) &= y_1(t) + y_2(t) \\ &= \int h_1(\tau)x(t-\tau)d\tau + \int\int h_2(\tau_1,\tau_2)x(t-\tau_1)x(t-\tau_2)d\tau_1\,d\tau_2 + \cdots \end{aligned} \tag{A.1}$$

where

$y_1(t), y_2(t)$ = linear and nonlinear component of the response, respectively,

$h_1(\tau)$ = impulse response function,

$h_2(\tau_1,\tau_2)$ = second-order impulse response function

For this expansion, Kac and Siegert (1947) have shown that the response $y(t)$ can be obtained as the sum of the standardized normal variates and its squares as follows:

$$y(t) = \sum_j (\beta_j\, Z_j + \lambda_j Z_j^2) \tag{A.2}$$

Here, the parameters β_j and λ_j are evaluated by finding the eigenfunction and eigenvalues of the integral equation given by

$$\int K(\omega_1,\omega_2)\, \psi_j(\omega_2)\, d\omega_2 = \lambda_j\, \psi_j(\omega_1) \tag{A.3}$$

where

$K(\omega_1,\omega_2)$ = $H(\omega_1,\omega_2)\sqrt{S(\omega_1)\, S(\omega_2)}$

$H(\omega_1,\omega_2)$ = second-order frequency response function

$S(\omega)$ = input spectral density function

$$\psi_j(\omega) = \text{ orthogonal eigenfunction } = \begin{cases} \int \psi_j(\omega)\psi_k^*(k)d\omega = 1 & \text{for } j = k \\ 0 & \text{otherwise} \end{cases}$$

Since $y(t)$ is represented in terms of a standardized normal random variable, the probability density function of $y(t)$ can be derived through the characteristic function of Eq. A.2. This method developed by Kac and Siegert is a novel and meticulous approach for deriving the probability density function of a second-order nonlinear response. Unfortunately, however, the probability density function cannot be obtained in closed form. It is also understood that the parameters β_j and λ_j in Eq. A.2 are evaluated from information of either the second-order impulse response function, $h(t_1, t_2)$ or the second-order frequency response function, $H(\omega_1, \omega_2)$.

APPENDIX B
ARSLOE WAVE DATA

The wave data used in the present study were obtained by the Coastal Engineering Research Center (CERC), U. S. Army, at its Field Research Facility, located at Duck, North Carolina. The Field Research Facility has a 550-meter-long research pier extending into the Atlantic Ocean, equipped with seven Baylor resistance-type wave gages (see Figure B.1). Extensive wave measurements were made at this site for two months in 1980 under the Atlantic Ocean Remote Sensing Land-Ocean Experiment (ARSLOE) project.

During October 23 – 25, an extratropical cyclone moved directly through the experimental area with wind speeds on the order of 10 – 15 meters/sec. Continuous wave records were taken by the CERC Field Research Facility during the storm. Statistical analysis of these records were carried out by Ochi et al. (1982) at the Coastal and Oceanographic Engineering Department, University of Florida. The wave data analyzed in the present study are those recorded at two locations D615 and D625 along the pier and one buoy (wave rider) F710 located offshore along the extended line of the pier. The location of the wave gages and wave riders as well as the average water depth measured on October 21 and 27 by CERC are given in Figure B.1.

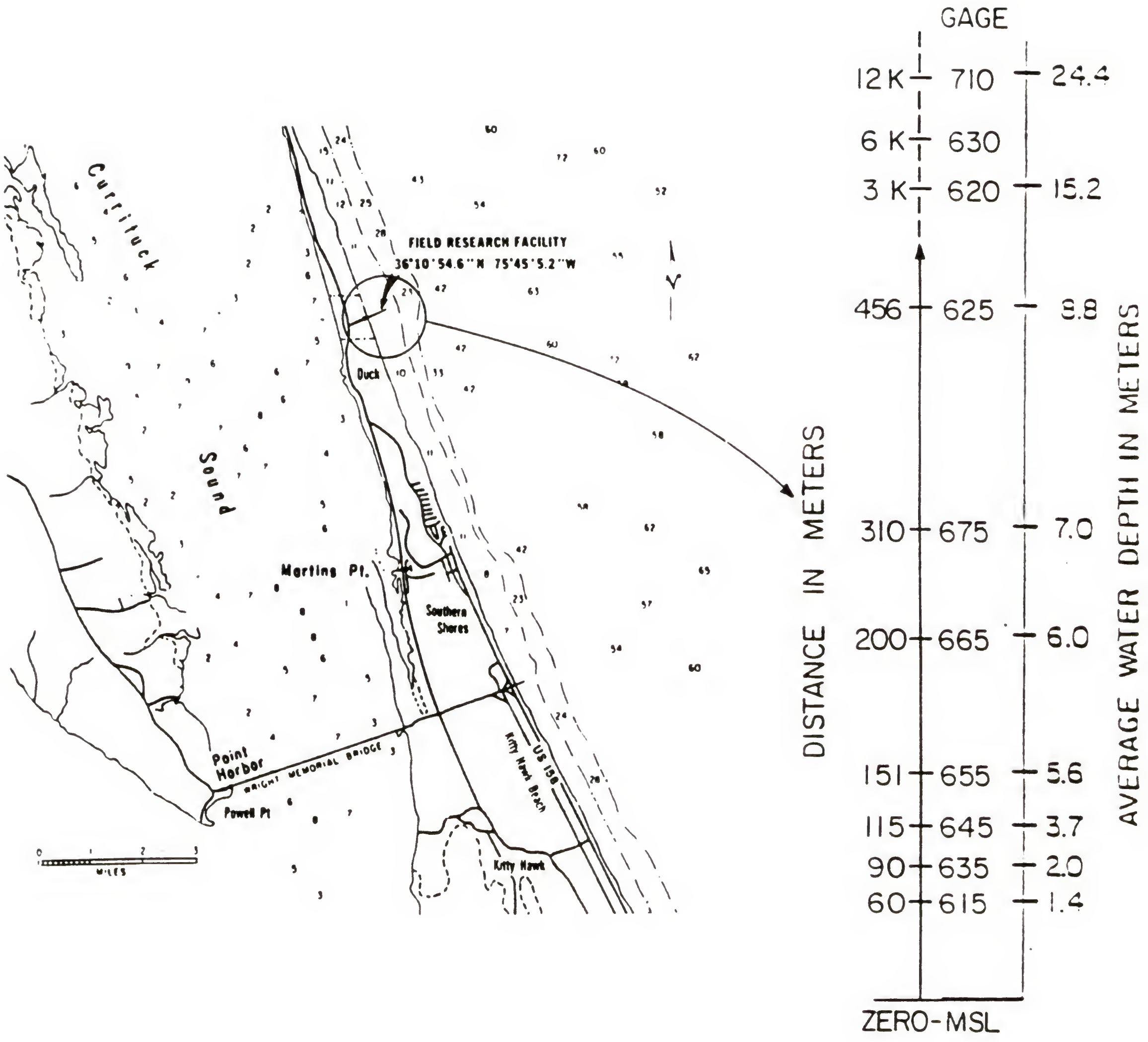

Figure B.1: Coastal Engineering Research Center (CERC) Field Research Facility, Duck, North Carolina (By courtesy of CERC)

APPENDIX C
COMPUTATION OF THE BISPECTRUM

This appendix outlines computational procedures of the bispectral estimation. Suppose that the water surface elevation, $y(t)$, is a sample of size N.

(1) Divide the total number of data points N into K sets of segments such that each segment has M data points.

$$y_j^{(k)} = y^{(k)}(j\Delta t), \quad k = 1, \ldots, K \text{ and } j = 1, \ldots, M \tag{C.1}$$

(2) Subtract the mean value from each segment.

(3) Apply an appropriate window function w_j to each segment to reduce leakage.

$$v_j = w_j\, y_j, \quad j = 1, \ldots, M \tag{C.2}$$

(4) Compute the complex Fourier coefficients by using FFT technique.

$$V_j^{(k)} = \frac{1}{M} \sum_{l=0}^{M-1} v_l\, e^{-i2\pi jl/M}, \quad j = 0, \ldots, \frac{M}{2} - 1 \tag{C.3}$$

One should scale $V_j^{(k)}$ to obtain the correct magnitudes (Bendat and Piersol, 1980).

$$Y_j^{(k)} = \frac{V_j^{(k)}}{\sqrt{\sum_{l=1}^{M} w_l^2}} \quad j = 1, \ldots, M \tag{C.4}$$

(5) Estimate the bispectrum and the bicoherence spectrum by averaging bispectral values from each segment (ensemble averaging).

$$\hat{B}(\omega_k, \omega_l) = \frac{1}{K} \sum_{i=1}^{K} X_k^{(i)} X_l^{(i)} X_{k+l}^{*(i)} \tag{C.5}$$

where " $\hat{B}$ " denotes an estimator and the bispectrum estimate obtained by arithmetic ensemble averaging is an unbiased, minimum variance estimator (Kim and Power, 1979).

For step 1 in the procedure, to achieve the smallest spectral variance from a fixed number of available sample data points, we divided the total number of data points $N = 2176$ (sampling frequency is 2 Hz) into segments of $M = 256$ points with 50 percent overlap of each segment. Therefore, the number of segments, K, is

$$K = \frac{N}{M/2} - 1 = \frac{2176}{128} - 1 = 16 \tag{C.6}$$

According to Welch (1967), the 50 percent overlap is nearly optimal to have the smallest variance. The overall reduction in variance is a factor of $11/(9K)$ compared to the variance of each realization, and the equivalent degrees of freedom (d.o.f.) of approximating chi-square distribution is

$$\text{d.o.f.} \approx 3.584 \frac{N}{M+1} = 3.584 \times \frac{2176}{256+1} = 30 \tag{C.7}$$

According to Elgar and Guza (1988),the 80 percent significance level for zero bicoherence for 30 degrees of freedom is approximaly 0.3. Therefore, bicoherence squared values greater than 0.09 are selected for the separation of second-order spectrum from the measured spectrum as explained in Chapter 3.2.

APPENDIX D
INVERSE PRESENTATION OF $Y = U + aU^2$

The functional relationship between two random variables Y and U is given in Eq. 4.22 as follows:

$$Y = U + aU^2 \tag{D.1}$$

where "a" is a constant and U is a normal variable with mean μ_* and variance σ_*^2. The probability density function of Y obtained by using the functional relationship vanished at a point $Y = -1/(4a)$ due to a singularity involved in the density function of Y. One way to solve this difficulty is to derive the density function of Y by presenting the functional relationship given in Eq. D.1 inversely such that the random variable U is expressed as a function of Y. For this, let us write Eq. D.1 in dimensionless form. That is

$$W = V + V^2 \tag{D.2}$$

where $W = aY$ and $V = aU$.

Then, we may write V as a function of W as follows:

$$V = \frac{1}{\gamma}(1 - e^{-\gamma W}) \tag{D.3}$$

where γ = constant.

Prior to determining the value of γ, let us find the domain of W and V appropriate for non-Gaussian random processes in practice. We consider first the positive domain of V and W. As an example, the random process shown in Figure 3.3, Gage No. D615 demonstrates a typical feature of non-Gaussian characteristics — a definite excess of high crests and shallow troughs. The skewness of this example is 1.03 which indicates a considerable deviation in the shape of the proability density function from that of a Gaussian process. In this example, the maximum positive deviation from the mean value is less than 2.1, and "a" is 0.37. Thus, the range of W from 0 to 0.78 (V from 0 to 0.51) appears to be sufficient for this example of a random process having strong nonlinearity.

As another example, let us consider the nonlinear turbulent wind- induced drag force on a structure. The instantaneous wind speed at height z above the sea surface can be written as

$$U_z = \overline{U}_z + w(t) \tag{D.4}$$

where $\overline{U}_z$ = mean wind speed at height z

$w(t)$ = turbulent wind speed.

The wind-induced drag force, F_D, acting on the structure with a projected area of A can be evaluated by

$$\begin{aligned} F_D &= \frac{1}{2}\,\rho\, C_D\, A\,\{\overline{U} + w(t)\}^2 \\ &\approx \frac{2\,\overline{F}_D}{\overline{U}}\, w(t) + \frac{\overline{F}_D}{\overline{U}^2}\, w(t)\,|w(t)| = a\,w + b\,w\,|w| \end{aligned} \tag{D.5}$$

where

ρ = air density

C_D = drag coefficient

$\overline{F}_D$ = drag force due to mean wind speed $\overline{U} = \frac{1}{2}\,\rho\, C_D\, A\, \overline{U}^2$

$a = 2\overline{F}_D/\overline{U}, \quad b = \overline{F}_D/\overline{U}^2$

By multiplying by (b/a^2) on both sides of Eq. D.5, we can present the drag force in the same dimensionless formula as given in Eq. D.2 with $W = F_D(b/a^2)$ and $V = (b/a)w$.

We may consider an extremely severe wind having a speed of 38.5 m/sec (75 knots) with a maximum turbulent speed of 30.8 m/sec (60 knots) blowing over a structure with a projected area of $2 \times 10^3\ m^2$. This results in a = 107×10^3 kg/m, and thereby we have a maximum V of 0.38. In other words, the range of V is from 0 to 0.35 and thereby W ranges from 0 to 0.47 yielding a much smaller domain of V and W than that obtained for the random process shown in Figure 3.3, Gage No. D615.

Next, let us choose the $\gamma-$ value in Eq. D.3 which yields the closest agreement with Eq. D.1 in the positive domain of W and V discussed above. Results of computation show that $\gamma = 1.28$ in Eq. D.3 as shown in Figure D.1 in the specified domain.

The negative domain of W and V is obtained through a method similar to that considered for the positive domain. For the non- Gaussian random processes shown in Figure 3.3 Gage No. D615, the smallest negative deviation from the mean value is less than -1.0, and thereby the range of W is from 0 and -0.37. Note that the probability density function of Y obtained by using Eq. D.1 has a singular point at $y = -1/(4a)$ and hence at $W = -ay = -0.25$. Therefore, it is appropriate to choose a $\gamma-$value in Eq. D.3 which best fits Eq. D.1 for W less than -0.25. The results of computation indicate that $\gamma = 3.00$ in Eq. D.3 as shown in Figure D.2 best represents Eq. D.1 in the specified range of W.

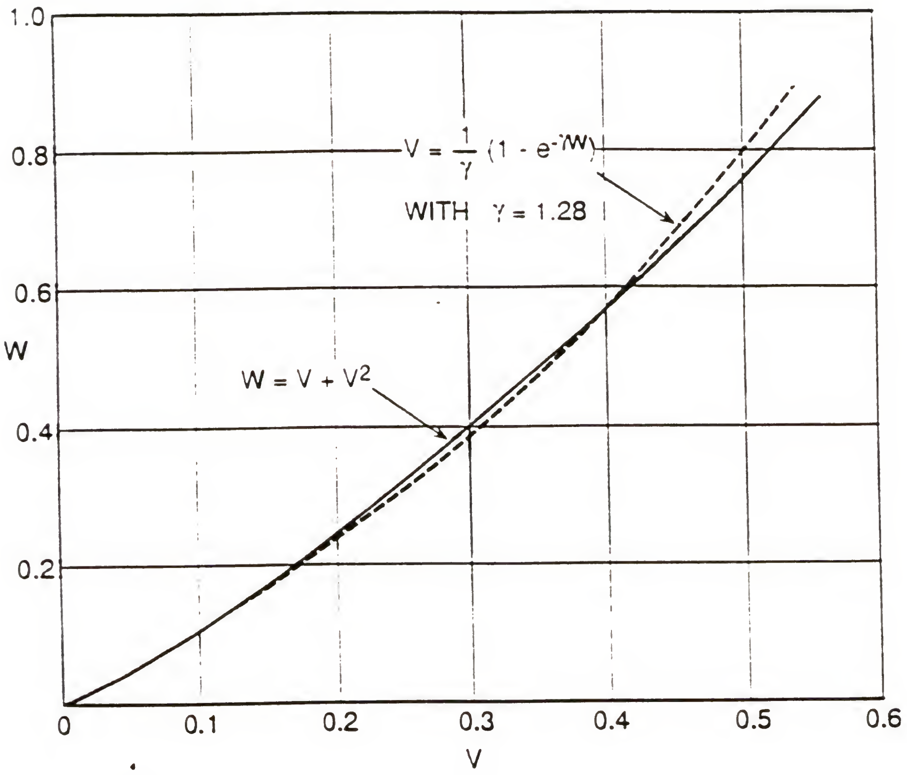

Figure D.1: Comparison between $W = V + V^2$ and $V = (1 - \exp\{-\gamma W\})/\gamma$ with $\gamma = 1.28$, $(V, W > 0)$

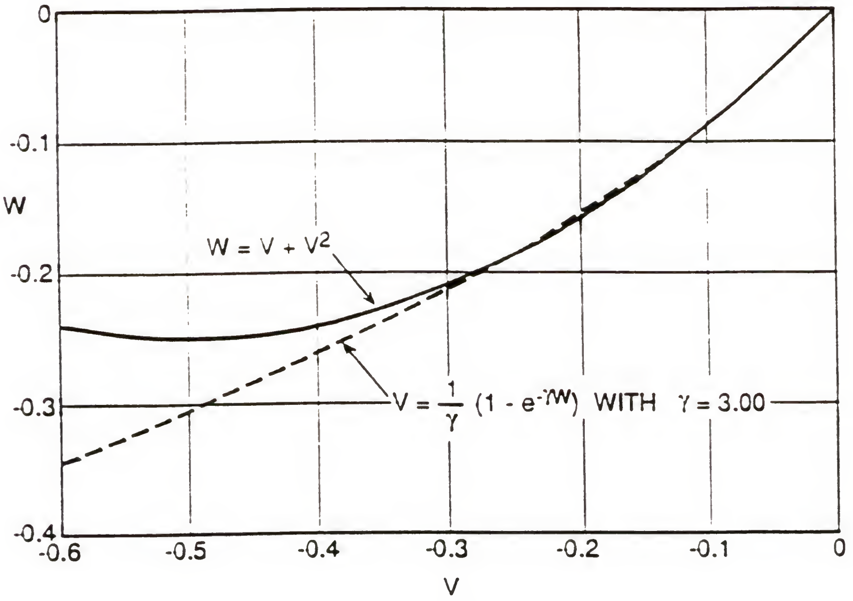

Figure D.2: Comparison between $W = V + V^2$ and $V = (1 - \exp\{-\gamma W\})/\gamma$ with $\gamma = 3.00$, $(V, W < 0)$

BIBLIOGRAPHY

Anastasiou, K., Tickell, R.G., and Chaplin, J.R., 1982, The Nonlinear Properties of Random Wave Kinematics, Proc. Third International Conference on the Behavior of Offshore Structures, M.I.T., Cambridge, Mass. Paper No. H7, pp. 493-515.

Bendat, J.S. and Piesol, A.G., 1980, Engineering Applications of Correlation and Spectral Analysis, Wiley-Interscience, New York.

Bowden, K.F., 1948, Some Observation of Waves and Other Fluctuations in a Tidal Current, Proc. Royal Society of London, A192, pp. 403-425.

Cieślikiewicz, W., 1990, Determination of the Surface Elevation Probability Distribution of Wind Waves Using Maximum Entropy Principle, Water Wave Kinematics (A. Torum and O.T. Gudmestad, Eds.), Kluwer Academic Publishers, Printed in the Netherlands, pp. 345-348.

Dowson, D.C. and Wragg, A., 1973, Maximum-Entropy Distribution Having Prescribed First and Second Moments, IEEE Trans. Information Theory, Vol. IT-19, pp. 689-693.

Edgeworth, F.Y., 1905, The Law of Error, Trans. Cambridge Philosophical Society, Vol. 20, pp. 36-65.

Elgar, S. and Guza, R.T., 1988, Statistics of Bicoherence, IEEE Transactions on Acoustics, Speech, and Signal Processing, Vol. 36, pp. 1667-1668.

Hamada, T., 1965, The Secondary Interactions of Surface Waves, Rep. Port and Harbour Research Institute, No. 10, pp. 1-28.

Hasselmann, K., 1962, On the Nonlinear Energy Transfer in a Gravity Wave Spectrum, Part 1, General, J. Fluid Mechanics, Vol. 12, pp. 481-500.

Hasselmann, K., 1963a, On the Nonlinear Energy Transfer in a Gravity Wave Spectrum, Part 2, Conservation Theorems, Wave Particle Correspondence, Irreversibility, J. Fluid Mechanics, Vol. 15, pp. 273-281

Hasselmann, K., 1963b, On the Nonlinear Energy Transfer in a Gravity Wave Spectrum, Part 3, Computation of the Energy Flux and Swell-Sea Interaction for a Neumann Spectrum, J. Fluid Mechanics, Vol. 15, pp. 383-398.

Huang, N.E., Long, S.R., Tung, C.C., and Yuan, Y., 1983, A Non-Gaussian Statistical Model for Surface Elevation of Nonlinear Random Wave Fields, J. Geophysical Research, Vol. 88, No. C12, pp. 7597-7606.

Hudspeth, R.T. and Chen, M.C., 1979, Digital Simulation of Nonlinear Random Waves, J. Waterways, Port, Coastal and Ocean Div., Proc. American Society of Civil Engineers, Vol. 105, No. WW1, pp. 67-85.

Jaynes, E.T., 1957, Information Theory and Statistical Mechanics, Physical Review, Vol. 106, No. 4, pp. 620-630.

Kac, M. and Siegert, A.J.F., 1947, On the Theory of Noise in Radio Receivers with Square Law Detectors, J. Applied Physics, Vol. 8, pp. 383-397.

Kim, Y.C. and Power, E.J., 1979, Digital Bispectral Analysis and its Applications to Nonlinear Wave Interactions, IEEE Trans, Plasma Science, Vol. PS-7, No. 2, pp. 120-131.

Kinsman, B., 1960. Surface Waves at Short Fetches and Low Wind Speed–a Field Study. Chesapeake Bay Inst. Tech. Rep. No. 19.

Langley, R.S., 1987. A Statistical Analysis of Nonlinear Random Waves. Ocean Engineering, Vol. 14, No 5, pp. 389-407.

Longuet-Higgins, M.S., 1963. The Effect of Nonlinearities on Statistical Distributions in the Theory of Sea Waves. J. Fluid Mechanics, Vol. 17, pp. 459-480.

Masuda, A., Kuo, Y., and Mitsuyasu, H., 1979, On the Dispersion Relation of Random Gravity Waves. Part 1. Theoretical Framework, J. Fluid Mechanics, Vol. 92, Part 4, pp. 717-730.

Ochi, M.K., 1985, Non-Gaussian Random Processes in Ocean Engineering, J. Probabilistic Engineering Mechanics, Vol. 1, No. 1, pp. 28-39.

Ochi, M.K., Malakar, S.B., and Wang, W.C., 1983, Statistical Analysis of Coastal Waves Observed During the ARSLOE Project, UFL/COEL/TR-045, Coastal and Oceanographic Engineering Department, U. of Florida, Gainesville.

Ochi, M.K. and Wang, W.C., 1984a, Prediction of Wind-Generated Seas in Finite Water Depth, UFL/COEL/TR-052, Coastal and Oceanographic Engineering Department, U. of Florida, Gainesville.

Ochi, M.K. and Wang, W.C., 1984b, Non-Gaussian Characteristics of Coastal Waves, Proc. 19th International Conference on Coastal Engineering, Houston.

Phillips, O.M., 1960. On the Dynamics of Unsteady Gravity Waves of Finite Amplitude. Part 1. The Elementary Interactions, J. Fluid Mechanics, Vol. 9, pp. 193-217.

Phillips, O.M., 1961. On the Dynamics of Unsteady Gravity Waves of Finite Amplitude. Part 2. Local Properties of a Random Wave Field, J. Fluid Mechanics, Vol. 11, pp. 143-155.

Sharma, J.N. and Dean, R.G., 1979, Development and Evaluation of a Procedure for Simulating a Random Directional Second Order Sea Surface and Associated Wave Forces, Ocean Engineering Report No. 20, University of Delaware, Newark, Del.

Sobczyk, K. and Trebicki, J., 1990, Maximum Entropy Principle in Stochastic Dynamics, Probabilistic Engineering Mechanics, Vol. 5, No. 3, pp. 102-110.

Tayfun, M.A., 1980, Narrow-Band Nonlinear Sea Waves, J. Geophysical Research, Vol. 85, No. C3, pp. 1548-1552.

Tick, L.J., 1959, A Nonlinear Random Model of Gravity Waves I, J. Mathematics and Mechanics, Vol. 8, pp. 184-196.

Tick, L.J., 1961, Nonlinear Probability Models of Ocean Waves, Proceedings of a Conference on Ocean Wave Spectra, Easton, Md., pp. 163-169.

Tuah, H. and Hudspeth, R.T., 1985, Finite Water Depth Effects on Nonlinear Waves, J. Waterways, Port, Coastal and Ocean Div., Proc. American Society of Civil Engineers, Vol. 111, No. 2, pp. 401-416.

Welch, P.D., 1967, The Use of Fast Fourier Transform for the Estimation of Power Spectra: A Method Based on Time Averaging Over Short, Modified Periodograms, IEEE Trans. Audio and Electroacoustics, Vol. AU-15, pp. 70-73.

BIOGRAPHICAL SKETCH

The author was born April 27, 1957, in Seoul, Korea. He grew up in a college town located in the suburban area of Seoul, where his father was a professor teaching hydraulics and coastal engineering in the Civil Engineering Department. When not attending school, the author spent much of his time drawing figures, playing Go (an oriental game played between two players who alternately place black and white stones on a board), collecting stamps, swimming and fishing in a small pond.

Following graduation from Seoul National University with a B.S. degree in civil engineering, the author spent 26 months in the Korean Army to fulfill his military duty. It was during this period that he discovered his deep desire to become a scholar.

After being discharged from the Korean Army, he came to the United States to study hydraulics at the Iowa Institute of Hydraulics Research, University of Iowa, from which he received an M.S. degree in 1986. In 1987, the author moved to Florida to continue his education in coastal engineering. At the University of Florida, he earned an M.E. degree in oceanographic engineering in 1989 and now he is a Ph.D. candidate in the Coastal and Oceanographic Engineering Department. During his stay in the United States, the most important event in his life happened in March 1991. That is, he became a born-again Christian! Now, the author is a happy believer.

I certify that I have read this study and that in my opinion it conforms to acceptable standards of scholarly presentation and is fully adequate, in scope and quality, as a dissertation for the degree of Doctor of Philosophy.

Michel K. Ochi

Michel K. Ochi, Chairman
Professor of Coastal and Oceanographic
Engineering

I certify that I have read this study and that in my opinion it conforms to acceptable standards of scholarly presentation and is fully adequate, in scope and quality, as a dissertation for the degree of Doctor of Philosophy.

D. Max Sheppard

D. Max Sheppard
Professor of Coastal and Oceanographic
Engineering

I certify that I have read this study and that in my opinion it conforms to acceptable standards of scholarly presentation and is fully adequate, in scope and quality, as a dissertation for the degree of Doctor of Philosophy.

DM Hanes

Daniel M. Hanes
Associate Professor of Coastal and
Oceanographic Engineering

I certify that I have read this study and that in my opinion it conforms to acceptable standards of scholarly presentation and is fully adequate, in scope and quality, as a dissertation for the degree of Doctor of Philosophy.

Robert J. Thieke
Assistant Professor of Coastal and
Oceanographic Engineering

I certify that I have read this study and that in my opinion it conforms to acceptable standards of scholarly presentation and is fully adequate, in scope and quality, as a dissertation for the degree of Doctor of Philosophy.

Ulrich Kurzweg

Ulrich H. Kurzweg
Professor of Aerospace Engineering,
Mechanics, and Engineering Science

This dissertation was submitted to the Graduate Faculty of the College of Engineering and to the Graduate School and was accepted as partial fulfillment of the requirements for the degree of Doctor of Philosophy.

August 1993

Winfred M. Phillips
Dean, College of Engineering

Dean, Graduate School